

THE LYMAN-CONTINUUM FLUXES AND STELLAR PARAMETERS OF O AND EARLY
B-TYPE STARS

035185

WILLIAM D. VACCA^{1,2}

Astronomy Department, 601 Campbell Hall, University of California, Berkeley, CA 94720

AND

CATHARINE D. GARMANY^{3,4} AND J. MICHAEL SHULL^{4,5}

Joint Institute for Laboratory Astrophysics, University of Colorado and National Institute of Standards and Technology, Campus Box 440, Boulder, CO 80309

Received 1995 January 30; accepted 1995 August 22

ABSTRACT

Using the results of the most recent stellar atmosphere models applied to a sample of hot stars, we construct calibrations of effective temperature (T_{eff}), and gravity ($\log g$) with a spectral type and luminosity class for Galactic O-type and early B-type stars. From the model results we also derive an empirical relation between the bolometric correction and T_{eff} and $\log g$. Using a sample of stars with known distances located in OB associations in the Galaxy and the Large Magellanic Cloud, we derive a new calibration of M_V with spectral class. With these new calibrations and the stellar atmosphere models of Kurucz, we calculate the physical parameters and ionizing photon luminosities in the H^0 and He^0 continua for O and early B-type stars. We find substantial differences between our values of the Lyman-continuum luminosity and those reported in the literature. We also discuss the systematic discrepancy between O-type stellar masses derived from spectroscopic models and those derived from evolutionary tracks. Most likely, the cause of this "mass discrepancy" lies primarily in the atmospheric models, which are plane parallel and hydrostatic and therefore do not account for an extended atmosphere and the velocity fields in a stellar wind. Finally, we present a new computation of the Lyman-continuum luminosity from 429 known O stars located within 2.5 kpc of the Sun. We find the total ionizing luminosity from this population ($Q_0^{\text{tot}} = 7.0 \times 10^{51}$ photons s^{-1}) to be 47% larger than that determined using the Lyman continuum values tabulated by Panagia.

Subject headings: Stars: atmospheres — stars: early-type — stars: fundamental parameters — ultraviolet: stars

1. INTRODUCTION

A basic ingredient of photoionization models of H II regions and starburst galaxies is the Lyman continuum (LyC) photon luminosity produced by massive stars. The classic paper on this subject is that by Panagia (1973), who used the temperature scale of Conti (1973), the absolute magnitude scale of Conti & Alschuler (1971), and a set of non-LTE and line-blanketed LTE model atmospheres (Auer & Mihalas 1972; Hickock & Morton 1968; Bradley & Morton 1969; Van Citters & Morton 1970) to calculate hydrogen ionizing luminosities (Q_0) and other stellar parameters for stars with spectral types between O4 and B3 and luminosity classes V, III, and I, as well as for objects on the zero-age main sequence (ZAMS). These values have been generally accepted as the standard parameters in the literature. A more recent tabulation of the ionizing fluxes from O stars has been given by Leitherer (1990), who used the luminosity and temperature calibrations of Schmidt-Kaler (1982) and the line-blanketed LTE models of Kurucz (1979) in his calculations.

Since Panagia's (1973) tabulation of LyC photon luminosities, both observations and theoretical models of the

atmospheres of hot stars have improved considerably. The recent stellar atmosphere models of B to K-type stars calculated by Kurucz (1992; see also Castelli & Kurucz 1994) and the models for O-type stars, beginning with the work of Kudritzki (1980) and including the results of Voels et al. (1989), Bohannan et al. (1990), Kudritzki et al. (1991), Grigsby, Morrison, & Anderson (1992), and Herrero et al. (1992), among others, represent substantial improvements over earlier attempts to reproduce observed stellar spectra. In addition, the spectral classification system has been extended and refined. Even the accepted value of the bolometric luminosity of the Sun has changed since the papers of Panagia (1973) and Schmidt-Kaler (1982); this value sets the zero point of the scales for both the bolometric luminosity and the bolometric correction. Therefore, we believe that new calculations of the LyC luminosities and stellar parameters of OB stars are timely. We have followed a procedure similar to that of Panagia (1973) in order to calculate these values. Using the results of the recent spectral modeling of a large sample of hot stars, we have determined new empirical calibrations of stellar parameters with spectral class. Then, employing a large grid of theoretical spectra derived from the latest atmosphere models available, we have derived a new set of LyC fluxes.

In § 2, we present our new calibrations for the effective temperature T_{eff} , stellar gravity $\log g$, bolometric correction BC, and absolute visual magnitude M_V . In § 3, we describe the methods used to determine the stellar bolometric luminosity L , radius R , mass M , and the H^0 and He^0 ionizing photon fluxes (q_0 and q_1 , respectively) from our adopted

¹ Hubble and Beatrice Watson Parrent Fellow.

² Currently at the Institute for Astronomy, 2680 Woodlawn Drive, Honolulu, HI 96822; vacca@galileo.ifa.hawaii.edu.

³ garmany@jila.colorado.edu.

⁴ Also at the Center for Astrophysics and Space Astronomy, Department of Astrophysical, Planetary, and Atmospheric Sciences, University of Colorado.

⁵ mshull@casa.colorado.edu.



calibrations and the latest model atmospheres of Kurucz (1992; Castelli & Kurucz 1994). In § 4, we present our results. We provide tables of the basic physical stellar parameters and the H^0 and He^0 ionizing photon luminosities (Q_0 and Q_1 , respectively) for massive stars with spectral types O3–B0.5 and luminosity classes V (dwarf), III (giant), and Ia (supergiant). In addition, we discuss the “mass discrepancy” problem encountered when comparing results from spectroscopic analyses of hot stars with those derived from current evolutionary models. Finally, we use our LyC values to estimate the total LyC luminosity produced by a sample of O-type stars located within 2.5 kpc of the Sun. Our results are summarized in § 5.

2. STELLAR CALIBRATIONS

In order to determine fundamental quantities representative of the various types of O and B stars, a method of converting stellar spectral classifications into physical parameters is needed. Below we present three such calibrations of physical quantities with spectral class. Two of these have been derived from the results of detailed modeling of the observed absorption line spectra of a number of stars with well-defined spectral classifications (i.e., spectral types and luminosity classes). The fourth calibration derived below relates quantities determined from the spectroscopic models to one another. Descriptions of the current generation of H and He non-LTE, plane-parallel, hydrostatic model atmospheres used to analyze O star spectra can be found in a number of references (e.g., Kudritzki 1976, 1980; Abbott & Hummer 1985; Bohannan et al. 1986; Voels et al. 1989). The models have been thoroughly reviewed by Kudritzki & Hummer (1990, hereafter referred to as KH90) and Kudritzki et al. (1991), and we refer readers to these papers and the references therein. The models continue to be improved, and a number of important effects have recently been incorporated, such as spherical extension, wind blanketing and emission, metal opacities, and line blanketing (Gabler et al. 1989; Kunze, Kudritzki, & Puls 1992; Sellmaier et al. 1993; Herrero 1994). Non-LTE line-blanketed hydrodynamic models, incorporating spherically expanding winds, have been developed independently by Schaerer & Schmutz (1994). However, these newer models have yet to be applied to the analysis of large numbers of stars. Therefore, we will rely on the results of the “older” models.

With the current generation of plane-parallel, hydrostatic, non-LTE models of hot stars, a successful fit to an observed O star spectrum requires (at least) four fundamental parameters: the effective temperature T_{eff} , the gravity $\log g$, the helium abundance by number y , and the line-of-sight component of the rotation velocity $v \sin i$ (see, e.g., Voels et al. 1989; Herrero et al. 1992). The more sophisticated models incorporating stellar winds and spherical extension require, in addition, a description of the structure of the wind, in terms of mass-loss rate, density profile, and velocity field (Gabler et al. 1989; Sellmaier et al. 1993; Schaerer & Schmutz 1994). We will not be concerned with the helium abundance in this paper and will assume that the determinations of the remaining stellar parameters (T_{eff} , $\log g$, and $v \sin i$) are not greatly affected by variations in the value of y . In fact, we will assume that all Galactic O-type stars discussed here have the same value of y . (We adopt $y = 0.1$.) The rotation velocity will be used only to make small corrections to $\log g$ to account for the centrifugal force in rapidly rotating stars. With the values of T_{eff} and $\log g$

derived from the models for a sample of stars with well-defined spectral classifications, we can then calibrate these quantities as a function of spectral type and luminosity class. In addition, we can derive the relationship between the bolometric corrections determined from the models and the values of T_{eff} and $\log g$. As pointed out by KH90, the spectra of hot stars are sensitive functions of *both* T_{eff} and $\log g$; therefore, *both* parameters are needed to provide a complete description of any O or early B-type star.

The final calibration needed for this work is that of absolute visual magnitude, M_V , with spectral class. When combined with the bolometric correction, the M_V yields the luminosity L of a star. With the values of T_{eff} , $\log g$, and L in hand for each spectral class, we can derive the remaining physical parameters (e.g., R , M , Q_0 , and Q_1) from stellar atmosphere models.

Before deriving our own set of calibrations below, we discuss a number of the calibrations for hot stars that can be found in the literature. More extensive discussions of various calibrations, as well as tabulations of fundamental physical parameters of O-type stars, can be found in the reviews by Divan & Burnichon-Prévoit (1988) and Conti (1988).

2.1. T_{eff} Calibration

2.1.1. Previous Calibrations

A number of temperature calibrations for O-type stars can be found in the literature, occasionally presented as part of a compilation of stellar physical parameters. Usually, the calibrations provide T_{eff} for each spectral type for the three main luminosity classes (V, III, and I). Here we review several of the most commonly cited calibrations and discuss the relationships among them. A graphical comparison of the calibrations discussed here is presented in Figure 1 for luminosity class V.

The temperatures listed for O-type stars by Panagia (1973) were based on Conti’s (1973) calibration, which in turn was derived from a comparison of measured equivalent

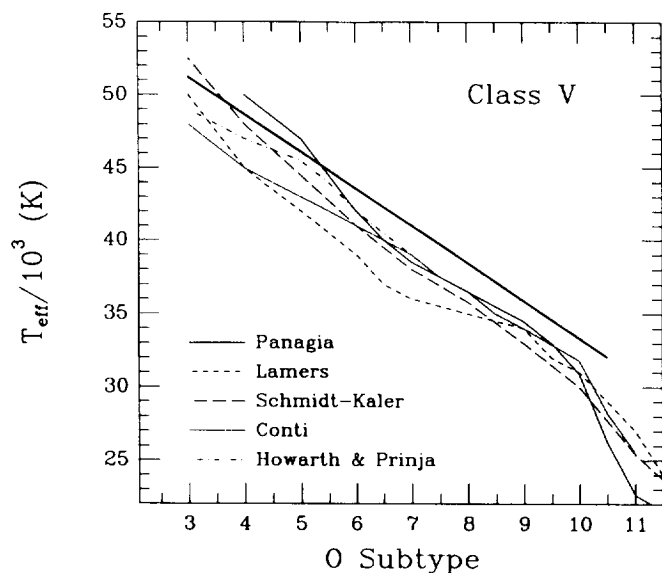


FIG. 1.—A comparison of the various spectral type– T_{eff} calibrations found in the literature for O and early B stars of luminosity class V. Subtypes 10 and greater refer to B stars. The different types of lines denote the calibrations of Panagia (1973) (and Conti 1973, 1975), Lamers (1981), Schmidt-Kaler (1982), Conti (1988), and Howarth & Prinja (1989). The heavy solid straight line represents the calibration derived in this paper; see § 2.1.2.

widths of He absorption lines in O star spectra with equivalent widths predicted from the non-LTE model atmospheres of Auer & Mihalas (1972). Conti (1973, 1975) discussed the difficulties associated with previous temperature determinations of hot stars, and his use of spectral lines represented a fundamental advance in the temperature determinations for these stars. An alternative, independent method of deriving effective temperatures and angular diameters from integrated flux measurements was discussed by Lamers (1981) and Remie & Lamers (1982). The calibrations of T_{eff} as a function of spectral type presented by Lamers (1981) and Conti (1975) are in agreement at subtype O9 but diverge for earlier spectral types. At the O3 subtype, Conti's scale is about 10% hotter.

Schmidt-Kaler (1982) included effective temperatures in his extensive compilation of stellar parameters. He adopted a temperature calibration for O stars based on the results of Conti (1975), Lamers (1981), and Kudritzki (1980). Kudritzki (1980) compared non-LTE model atmosphere calculations of H and He lines profiles with those measured from high-dispersion spectrograms for HD 93250 (O3 V) and derived a T_{eff} midway between the scales of Conti (1975) and Lamers (1981). The method of fitting line profiles used by Kudritzki (1980) has become the primary source of new temperature determinations for O-type stars (e.g., Voels 1989; Herrero et al. 1992).

Conti (1988) also presented a revised temperature calibration based on values of T_{eff} determined from various methods. The revised scale is nearly identical to his earlier scale (Conti 1975) between subtypes O6.5 and B1; for subtypes earlier than O6.5, the revised calibration predicts temperatures several thousand degrees lower than those of the earlier calibration.

While recognizing that the stellar atmosphere models did not yet incorporate all the relevant physics, Howarth & Prinja (1989) based their temperature calibration on the available non-LTE spectroscopic analyses of individual stars. After adjusting values for the effects of wind blanketing (using the model results presented by Abbott & Hummer 1985 and Bohannan et al. 1986), they required the temperature scale to be a smooth, monotonic function of spectral type and luminosity class. This scale differs little from that of Conti (1973) for stars later than O5.5.

2.1.2. A New T_{eff} Calibration

In order to derive a calibration of T_{eff} with spectral class, we require a sample of early-type stars that have been analyzed in a consistent manner, with similar models, and that span a wide range of spectral classes. Our proposed calibration is based on the results of the most recent non-LTE spectroscopic analyses of individual Galactic O-type and early B-type stars. The stars included in our sample were drawn from Table 1 of KH90 and the papers by Lennon et al. (1991a, b), Kolb (1991), Herrero et al. (1992), and Herrero (1994).⁶ The effective temperatures and gravities for these stars were derived by comparing the observed H and He line profiles in high-resolution optical spectra with the predictions from non-LTE, plane-parallel hydrostatic atmospheric models of hot stars. (See, e.g.,

KH90, Voels et al. 1989, or Herrero et al. 1992 for a description of the models and the exact procedures used.) We excluded results obtained from models that incorporate wind blanketing, since the quantitative effects of wind blanketing are uncertain at present. Furthermore, only a small fraction of the stars in our sample have been analyzed with models incorporating wind blanketing. However, it should be noted that temperatures determined from wind-blanketed models are significantly lower than those derived from unblanketed models. We also excluded stars in the Magellanic Clouds from our sample in order to avoid possible systematic differences in the temperature determinations owing to the effects of metallicity variations.

The 58 stars in our sample are listed in Tables 1–3, along with their adopted spectral types, effective temperatures T_{eff} , gravities $\log g$, and bolometric corrections BC. In most cases, whenever two sets of parameter values were available for a single star (resulting from two attempts to model the spectrum), we chose the values corresponding to the more recent analysis. For HD 46150, we used the weighted average of the values obtained by Imhoff (1990) and Herrero et al. (1992) while for HD 46966, we used the weighted average of the results of Imhoff (1990), Kolb (1991), and Herrero et al. (1992). For HD 34078, we averaged the non-wind-blanketed results from Voels et al. (1989) and Herrero et al. (1992); for HD 46223, we took the weighted average of the non-wind-blanketed results from Imhoff (1990) and Bohannan et al. (1990). Uncertainties on the individual values of the temperature and gravity were taken directly from the results of the spectroscopic analyses. For HD 34078, HD 46233, and HD 46966, we adopted the errors of the mean values for both quantities. For HD 46150, the two reported sets of temperature and gravity estimates are separated by an amount larger than the error ranges; in this case it seemed more reasonable to use the standard deviations rather than the errors of the means.

To construct an accurate calibration of parameters as a function of spectral class, consistent spectral classifications are crucial. Nearly all the stars in the sample have been classified in various papers by Walborn (1971, 1972, 1973, 1976, 1982), and we adopted his spectral classifications whenever possible. The classifications systems of Conti (Conti & Alschuler 1971; Conti & Leep 1974; Conti & Frost 1977) and Mathys (1988, 1989) yield similar spectral classifications for most stars.

A plot of effective temperature versus spectral type for the stars in our sample is presented in Figure 2. Effective temperature is clearly correlated with spectral type; a variation with luminosity class is also apparent for spectral types O6 and later. To derive a calibration for T_{eff} , we assumed that the effective temperature is a function of both spectral type and luminosity class with the form

$$T_{\text{eff}} = A + B \times S + C \times L_c + D \times S \times L_c, \quad (1)$$

where S is the numerical spectral type (between 3 and 10.5 for luminosity classes Ib–V and between 3 and 9.7 for luminosity class Ia; see below) and L_c is the numerical luminosity class (between 1 and 5). Higher order functions are not justified, given the scatter and the error bars on the data points.

We fitted the data points using a multidimensional least-squares routine. This allowed us to use all the stars in the sample to determine the best-fit values of the coefficients in the assumed relation. In performing the fit, we assigned a numerical luminosity class (L_c) value of 1.0 to stars with

⁶ Of the references given in Table 1 of KH90, we selected the results from Kudritzki (1980), Simon et al. (1983), Schönberner et al. (1988), Kudritzki et al. (1989), Voels (1989), Voels et al. (1989), Bohannan et al. (1990), Herrero, Vilchez, & Kudritzki (1990), and Imhoff (1990). Values from other references listed in Table 1 of KH90 have been superseded by more recent results.

TABLE 1
STELLAR SAMPLE—LUMINOSITY CLASS V

Star	Spectral Classification	Reference	T_{eff} (10^3 K)	$\log g$ (cgs)	BC (mag)	Reference
HD 93250	O3 V((f))	W72	51.0 ± 1.5	3.90 ± 0.10	-4.67	KH90
HDE 303308	O3 V((f))	W72	48.0 ± 1.5	3.91 ± 0.01	-4.29	KH90
HD 93128	O3 V((f))	W73	52.0 ± 1.5	3.91 ± 0.10	-4.44	KH90
HD 164794	O4 V((f))	W72	47.0 ± 1.0	3.90 ± 0.15	-3.97 ^a	KH90
HD 46223	O4 V((f))	W72	49.3 ± 0.8	3.95 ± 0.08	-4.18 ^a	Avg.
HD 168076	O4 V((f))	W73	50.5 ± 1.5	3.95 ± 0.10	...	KH90
HD 46150	O5 V((f))	W72	46.9 ± 3.5	3.85 ± 0.15	-4.05	Avg.
HD 15629	O5 V((f))	W72	47.0 ± 1.0	3.76 ± 0.10	-3.93	H94
HD 168075	O6 V((f))	W82	49.0 ± 1.5	3.95 ± 0.10	...	KH90
BD + 60° - 513	O7 Vn	W73	40.0 ± 1.5	3.70 ± 0.15	-3.30	KH90
HD 217086	O7 Vn	W73	40.0 ± 1.5	3.77 ± 0.10	-3.81	H92
HD 47839	O7 V((f))	W72	39.5 ± 1.0	3.71 ± 0.10	-3.77	H92
HD 46966	O8 V	W72	38.1 ± 0.6	3.89 ± 0.06	-3.62	Avg.
HD 48279	O8 V	W73	37.5 ± 1.5	4.01 ± 0.20	...	KH90
HD 168137	O8 V	HM69	40.0 ± 1.5	4.00 ± 0.10	...	KH90
HD 14633	ON8 V	W72	35.5 ± 1.5	3.72 ± 0.20	...	KH90
HD 13268	ON8 V	M89	35.0 ± 1.5	3.42 ± 0.10	-3.41	H92
NGC 6611 - 166	O9 V	HM69	37.5 ± 1.5	3.75 ± 0.10	...	KH90
HD 214680	O9 V	W72	37.5 ± 1.0	4.00 ± 0.10	-3.57	H92
HD 149757	O9 V(e)	CL74	32.5 ± 1.5	3.77 ± 0.10	-3.19	H92
NGC 6611 - 367	O9.5 V	HM69	35.0 ± 1.5	4.15 ± 0.10	...	KH90
HD 34078	O9.5 V	W72	36.0 ± 0.7	4.02 ± 0.08	-3.45 ^b	Avg.
HD 227757	O9.5 V	Hi56	36.0 ± 1.0	4.00 ± 0.10	-3.46	H92
HD 93521	O9.5 V	Ho82	33.5 ± 1.5	3.95 ± 0.20	...	L91a
HD 149438	B0.2 V	W71	33.0 ± 1.0	4.15 ± 0.20	...	KH90
HD 93030	B0.2 Vp	W76	32.5 ± 1.5	4.16 ± 0.20	...	KH90
HD 228199	B0.5 V	Hu78	30.0 ± 1.5	3.91 ± 0.10	-3.04	H92

^a BC value taken from a wind-blanketed model.

^b Average BC value taken from two models (see text).

REFERENCES.—W72: Walborn 1972. KH90: Kudritzki & Hummer 1990, and references therein (including Bohannan et al. 1990). W73: Walborn 1973. Avg.: average of two values (see text). H94: Herrero 1994. W82: Walborn 1982. H92: Herrero et al. 1992. HM69: Hiltner & Morgan 1969. M89: Mathys 1989. CL74: Conti & Leep 1974. Hi56: Hiltner 1956. Ho82: Hobbs et al. 1982. L91a: Lennon et al. 1991a. W71: Walborn 1971. W76: Walborn 1976. Hu 78: Humphreys 1978.

luminosity class Ia, while Ib's were given the value of 1.5. Stars with luminosity classifications of simply I were assigned the L_c value of 1.0 for spectral types earlier than O6 (Ia and Ib classifications are not distinguished for these early subtypes) and 1.25 for later subtypes. The early B II-V stars were included in the fit by adding 10 to their numerical subtypes, so that B0 is 10, and B0.5 is 10.5. The two B stars with luminosity class Ia were excluded from the fits; as seen in Figure 2, as well as in the plots of $\log g$ and M_V as a

function of spectral type (see below), for the Ia luminosity class there is an abrupt and substantial change in the variations of the stellar parameters with spectral type at subtype B0. Therefore, our calibrations cannot be applied to luminosity class Ia stars with spectral types B0 and later.

The coefficients A , B , C , and D and their uncertainties are listed in Table 4; the T_{eff} calibrations resulting from the fit are shown for three luminosity classes in Figure 2. The rms deviation of the data points from the fit is about 1700 K.

TABLE 2
STELLAR SAMPLE LUMINOSITY CLASS II AND III

Star	Spectral Classification	Reference	T_{eff} (10^3 K)	$\log g$ (cgs)	BC (mag)	Reference
HD 193682	O5 III(f)	M89	43.5 ± 2.3	3.56 ± 0.10	-4.12	H92
HD 15558	O5 III(f)	W72	48.0 ± 1.0	3.76 ± 0.10	-3.81	H94
HD 227018	O6.5 III	CL74	41.0 ± 1.0	3.71 ± 0.10	-3.89	H92
HD 190864	O6.5 III(f)	W72	41.0 ± 1.0	3.56 ± 0.10	-3.91	H92
HD 93222	O7 III((f))	W72	38.5 ± 1.5	3.65 ± 0.10	...	KH90
HD 191612	O7.5 III(f)	CL74	40.0 ± 1.0	3.61 ± 0.10	-3.82	H92
HD 24912	O7.5 III(n)(f)	W72	36.0 ± 1.5	3.40 ± 0.10	-3.54	H92
HD 203064	O7.5 III:n(f)	W72	37.5 ± 1.5	3.62 ± 0.10	-3.62	H92
HD 191423	O9 III:n	W73	34.0 ± 1.5	3.68 ± 0.10	-3.31	H92
HD 89137	O9.5 III(n)p	W76	30.0 ± 1.5	3.33 ± 0.20	...	KH90
HD 34656	O7 II(f)	W72	39.0 ± 1.0	3.51 ± 0.10	-3.74	H92
HD 36486	O9.5 II	W72	33.0 ± 1.0	3.47 ± 0.15	-3.22	KH90
HD 16429	O9.5 II(n)	W73	31.5 ± 1.0	3.15 ± 0.10	-2.70	KH90
HD 227634	B0 II	W71	28.5 ± 1.0	3.23 ± 0.10	-2.86	H92

REFERENCES.—M89: Mathys 1989. H92: Herrero et al. 1992. W72: Walborn 1972. H94: Herrero 1994. CL74: Conti & Leep 1974. KH90: Kudritzki & Hummer 1990, and references therein (including Bohannan et al. 1990). W73: Walborn 1973. W76: Walborn 1976. W71: Walborn 1971.

TABLE 3
STELLAR SAMPLE—LUMINOSITY CLASS I

Star	Spectral Classification	Reference	T_{eff} (10^3 K)	$\log g$ (cgs)	BC (mag)	References
Cyg OB2-8A.....	O6 Ib(n)f)	W73	45.0 ± 1.0	3.56 ± 0.10	...	H94
HD 192639.....	O7 Ib(f)	W72	38.5 ± 1.0	3.37 ± 0.10	-3.74	H92
HD 193514.....	O7 Ib(f)	W72	38.0 ± 1.0	3.37 ± 0.10	-3.71	H92
HD 207198.....	O9 Ib-II	W72	34.0 ± 1.0	3.31 ± 0.10	-3.34	H92
HD 210809.....	O9 Iab	W72	33.0 ± 1.0	3.12 ± 0.10	-3.30	H92
HD 209975.....	O9.5 Ib	W72	32.5 ± 1.0	3.22 ± 0.10	-3.23	H92
HD 37742.....	O9.7 Ib	W72	32.0 ± 1.0	3.23 ± 0.10	-3.16 ^a	KH90
HD 18409.....	O9.7 Ib	W73	31.5 ± 1.3	3.17 ± 0.10	-3.15	H92
Cyg OB2-7.....	O3 If*	W73	51.5 ± 1.0	3.71 ± 0.10	...	H94
HD 93129A.....	O3 If*	W72	50.5 ± 1.3	3.76 ± 0.03	-4.16	KH90
HD 66811.....	O4 I(n)f	W72	47.0 ± 1.0	3.64 ± 0.10	-3.92 ^a	KH90
HD 15570.....	O4 If+	W72	49.0 ± 3.0	3.51 ± 0.15	-3.85	H94
HD 14947.....	O5 If+	W73	43.5 ± 1.0	3.48 ± 0.10	...	H94
HD 210839.....	O6 I(n)fp	W73	40.0 ± 1.0	3.50 ± 0.10	...	KH90
HD 30614.....	O9.5 Ia	W72	32.0 ± 1.0	3.02 ± 0.10	-2.96 ^a	KH90
HD 37128.....	B0 Ia	W71	26.0 ± 1.0	2.75 ± 0.10	...	KH90
HD 38771.....	B0.5 Ia	W71	25.0 ± 1.0	2.70 ± 0.10	...	L91b

^a BC value taken from a wind-blanketed model.

REFERENCES.—W73: Walborn 1973. H94: Herrero 1994. W72: Walborn 1972. H92: Herrero et al. 1992. KH90: Kudritzki & Hummer 1990, and references therein (including Bohannan et al. 1990). W71: Walborn 1971. L91b: Lennon et al. 1991b.

The relation given above is close to that obtained when a linear least-squares procedure incorporating errors on both T_{eff} and spectral type (assigning an error in spectral type of 0.5) is used to fit the effective temperature as a function of spectral type alone for each luminosity class. The effective temperatures we calculate for stars of specific spectral types and luminosity classes are presented in Tables 5–7.

In Figure 3 we present a comparison between our calibration of T_{eff} as a function of spectral type and the calibrations given by Panagia (1973) and Schmidt-Kaler (1982). We assumed that the effective temperatures given in these references for luminosity class I stars apply to the Iab subclass. On average, our T_{eff} values are 2000–3000 K larger

for any given spectral type. Of course, the scatter in the values of T_{eff} for the stars within a given subtype (see Fig. 2) is as large as the systematic differences between our calibration and those of Panagia (1973) and Schmidt-Kaler (1982).

It is useful to compare the T_{eff} values listed in Tables 1–3 with those derived from different types of models. This allows one to judge the uncertainties in both the temperature determinations of hot stars and our resulting spectral class–effective temperature calibration. Kilian et al. (1991) used models incorporating non-LTE line formation in LTE line-blanketed atmospheres to analyze a set of Galactic early B-type stars. A comparison of the results for the B0.2 V star τ Sco (= HR 6165 = HD 149438), the only star common to our sample and that of Kilian et al. (1991), reveals that the LTE line-blanketed atmosphere models yield a somewhat smaller effective temperature ($T_{\text{eff}} = 31,400$ K) and a higher gravity ($\log g = 4.24$) than the non-LTE unblanketed models. Grigsby et al. (1992) used non-LTE line-blanketed model atmospheres to analyze a sample of Galactic stars with spectral types between O9 and B2. A comparison of their results for T_{eff} with the values predicted from our empirical calibration reveals a significant discrepancy; for spectral types between O9 and B05, the values of T_{eff} derived by Grigsby et al. (1992) are substantially (between 2000 and 8000 K) smaller than those determined from the expression given in equation (1). There are two stars common to our sample and that of Grigsby et al. (1992): HD 214680 (10 Lac, O9 V) and HD 149438 (τ Sco, B0.2 V). For HD 214680, Grigsby et al. (1992) find $T_{\text{eff}} = 30,000$ K and $\log g = 4.00$, while Herrero et al. (1992) find $T_{\text{eff}} = 37,500$ K and $\log g = 4.00$. For HD 149438, Grigsby et al. (1992) find $T_{\text{eff}} = 30,500$ K and $\log g = 4.25$, while Schönberner et al. (1988) find $T_{\text{eff}} = 33,000$ K and $\log g = 4.15$. Clearly, there is a significant difference between the two types of models and analyses.

The addition of metal line opacities can significantly alter the temperature structure in a model stellar atmosphere. Models incorporating metals indicate that line blanketing results in Balmer lines whose cores are shallower than those

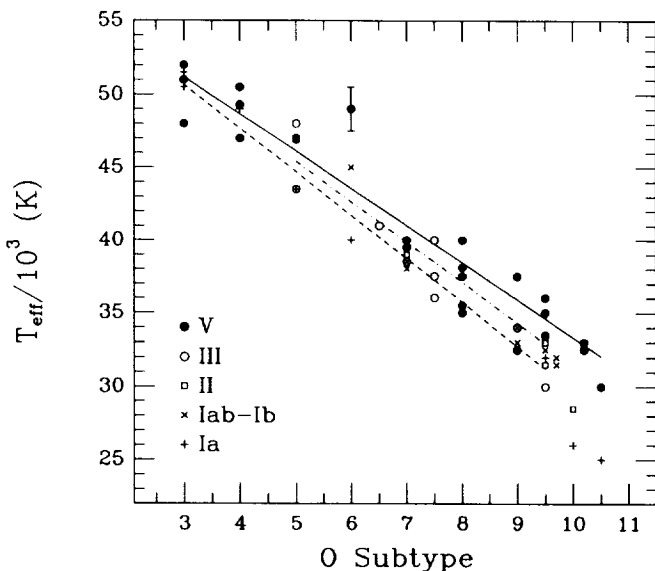


FIG. 2.—The variation of effective temperature, T_{eff} , with spectral subtype and luminosity class for the stars in the sample. A representative error bar is shown on one point. Subtypes 10 and greater refer to B stars. Lines denote the fits determined for three luminosity classes: the solid line is the best fit for luminosity class V stars; the dot-dashed line is for class III stars; the dashed line is for class Ia stars.

TABLE 4
COEFFICIENTS OF NUMERICAL FITS^a AND ASSOCIATED UNCERTAINTIES

$$x = A + B \times S + C \times L_c + D \times S \times L_c$$

<i>x</i>	<i>A</i>	σ_A	<i>B</i>	σ_B	<i>C</i>	σ_C	<i>D</i>	σ_D
T_{eff}^b	59.85	1.06	-3.10	0.14	-0.19	0.28	0.11	0.04
$\log g_{\text{spec}}^c$	4.095	0.056	-0.129	0.009	-0.037	0.012	0.025	0.002
$\log g_{\text{evol}}^d$	4.429	0.011	-0.140	0.002	-0.039	0.003	0.022	0.001
M_V	-6.320	0.316	-0.076	0.039	-0.026	0.078	0.060	0.010

^a *S* = Spectral type between 3 and 10.5 (for luminosity classes V–Ib) or between 3 and 9.5 (for luminosity class Ia); *L_c* = luminosity class between 1 and 5.

^b T_{eff} in units of 10^3 K.

^c Spectroscopic value, derived from the values determined from the spectroscopic analyses of the individual stars listed in Tables 1–3.

^d Evolutionary value, derived from interpolation in the evolutionary tracks; see text.

of unblanketed models, although the differences appear to be small (see, e.g., Werner 1988). When fitting the observed profiles of the Balmer lines, the unblanketed models may therefore yield effective temperatures which are slightly too high. On the other hand, the models used by Grigsby et al. (1992) tend to produce Balmer lines whose cores are deeper than those observed. Therefore, the effective temperatures derived by Grigsby et al. (1992) may be underestimated. In both types of non-LTE models (with and without line blanketing), the effects of wind emission and wind blanketing on the observed Balmer profiles have been neglected. Both effects are expected to reduce the derived effective temperatures. In general, the temperatures derived from the current generation of non-LTE model atmospheres may have substantial systematic uncertainties owing to the incomplete nature of the models.

2.2. *log g* Calibration

We used the same data sample and numerical procedures outlined above to derive a calibration for *log g* as a function of spectral type and luminosity class for OB stars. All values of *log g* have been corrected for the effects of rotation with the relation

$$g = g_{\text{eff}} + (v \sin i)^2/R, \tag{2}$$

where *g* is the true stellar gravity, g_{eff} is the effective gravity determined from the model fits to the observed line profiles, $v \sin i$ is the observed component of the stellar rotation velocity, and *R* is the stellar radius. Here we use the measured quantity, $(v \sin i)^2$, to approximate the centrifugal term, $(v \sin \theta)^2$, averaged over the stellar disk. The rotation velocity and radius values determined from the models were used to compute the correction term. In a few cases in which the radius was not given, we employed a calibration of radius with spectral type and luminosity class to estimate *R*. For some stars for which the rotation velocities determined from the most recent spectral fits were not reported, the values of $v \sin i$ were taken from earlier modeling attempts. We found the rotation velocities reported by various groups using different atmosphere models to be fairly consistent. In general, the correction for stellar rotation is very small and the approximate rotation velocity and radius values we used are more than adequate for our purposes.

The relation between the spectroscopic value of *log g* and the spectral type *S* and luminosity class *L_c* was assumed to be given by the expression

$$\log g = A + B \times S + C \times L_c + D \times S \times L_c, \tag{3}$$

and we determined the coefficients from a multidimensional

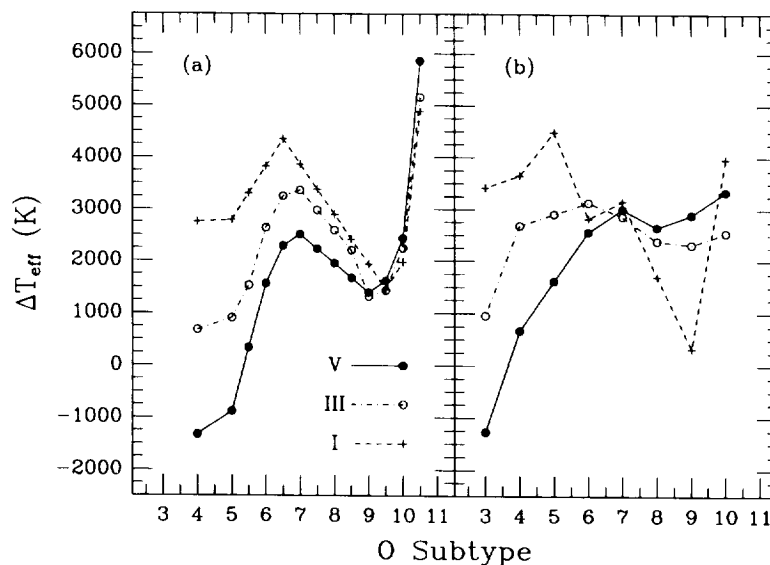


FIG. 3.—Comparison of the T_{eff} calibration derived in this paper with those given by (a) Panagia (1973) and (b) Schmidt-Kaler (1982) as a function of OB subtype for three luminosity classes. We assumed that the values given in the references for luminosity class I stars refer to the subclass Ia. Subtypes 10 and greater refer to B stars. Here $\Delta T_{\text{eff}} = T_{\text{eff}}$ (this paper) – T_{eff} (reference).

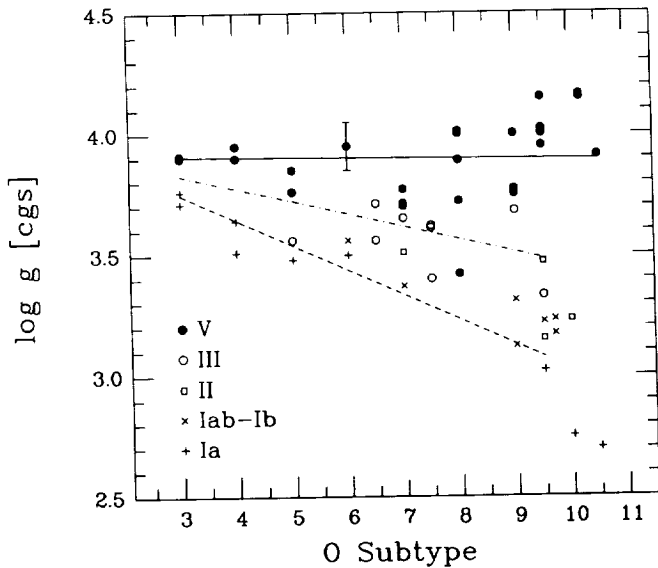


FIG. 4.—The variation of the stellar gravity, $\log g$, with spectral subtype and luminosity class for the stars in the sample. A representative error bar is shown on one point. Subtypes 10 and greater refer to B stars. Lines denote the fits determined for three luminosity classes: the solid line is the best fit for luminosity class V stars; the dot-dashed line is for class III stars; the dashed line is for class Ia stars.

fit to the values given in Tables 1–3. The results of our fit are presented in Figure 4, where a clear correlation between $\log g$ and luminosity class can be seen. The coefficients A , B , C , and D and their uncertainties are listed in Table 4. The rms deviation of the data points from the best fit is about 0.13 in $\log g$. The values of $\log g$ calculated for specific spectral types and luminosity classes are presented in Tables 5–7. (In Tables 4–7 the value of the gravity determined from this fit to the spectroscopic results is denoted as $\log g_{\text{spec}}$ in order to distinguish it from the value determined from the evolutionary models, $\log g_{\text{evol}}$. See § 3.)

We believe this is the first direct calibration of $\log g$ for O-type stars. Although Howarth & Prinja (1989) calculated values of $\log g$ for the various spectral types and luminosity classes, their values were derived from masses determined from evolutionary tracks and locations in the Hertzsprung-Russell (H-R) diagram. In § 4.3, we discuss at length the differences between the gravities determined from atmosphere models (spectroscopic analyses) and those derived from evolutionary models. It should be pointed out that the values of $\log g$ listed in Tables 1–3 were derived from models which do not account for possible contamination of the absorption line profiles by wind emission. Inclusion of this effect is expected to result in an increase in the derived stellar gravities. It may be necessary to redetermine the calibrations of T_{eff} and $\log g$ with spectral class when more complete models of hot stars become available.

2.3. Bolometric Corrections

Bolometric corrections for O star spectral types have been derived by a number of workers; usually BCs are provided along with a calibration of T_{eff} . The values given by Panagia (1973) were derived from the LTE atmosphere models of Morton (1969) and Van Citters & Morton (1970). The values given by Howarth & Prinja (1989) were derived by fitting the BCs determined from various LTE and non-LTE models (Morton 1969; Mihalas 1972; Kurucz 1979; Bohannan et al. 1986) as a linear function of T_{eff} . The values listed by Chlebowski & Garmany (1991) were based

on published results from the analysis of the observed spectra of 12 O stars with non-LTE stellar atmosphere models; they were derived by fitting the BC values for the individual stars as a linear function of $\log T_{\text{eff}}$. The stars used by Chlebowski & Garmany (1991) are included in the sample we used to determine a new relation between T_{eff} and BC.

For most of the stars in our sample, BCs could be derived or taken directly from the results of the spectroscopic analyses. For the stars taken from Herrero et al. (1990, 1992), the BCs were determined from the following equation:

$$\text{BC} = M_{\text{bol}, \odot} - 10 \log (T_{\text{eff}}/T_{\text{eff}, \odot}) - V - 29.57, \quad (4)$$

where $T_{\text{eff}, \odot}$ is the effective temperature of the Sun, taken to be 5777 K (Kurucz 1992), V is the integral over wavelength of the product of the theoretical stellar flux from the atmosphere models and the V filter function of Matthews & Sandage (1963), and the numerical constant is an absolute calibration value (Kudritzki 1980; Herrero et al. 1992). The value of the V integral is explicitly listed by Herrero et al. (1990, 1992). For stars taken from Voels et al. (1989) and Bohannan et al. (1990), we adopted the BCs calculated from the models and explicitly given in these papers. For HD 34078, we included two separate BCs derived from the results of Herrero et al. (1992) and Voels et al. (1989). In several cases, the reported BC values were derived from wind-blanketed models; in these cases we adopted the wind-blanketed values for T_{eff} and $\log g_{\text{eff}}$. In all cases, we adopted the effective temperature and effective gravity of the original model from which the BC was calculated; therefore, the BCs listed in Tables 1–3 may not necessarily correspond to the values of T_{eff} and $\log g$ given in these tables. We also included in our sample the BCs determined from 11 models calculated by Abbott & Hummer (1985).

We excluded the BCs determined by Herrero et al. (1990) for five stars (HD 15629, BD + 60 513, HD 15558, HD 16429, and HD 15570) from subsequent analysis. The BC values for these stars are all systematically about 0.5 mag larger than the values found for other stars (taken from other sources) with similar effective temperatures and gravities. The values of T_{eff} and $\log g$ listed by Herrero et al. (1990) for these stars, however, seem to be consistent with other objects with the same spectral types and luminosity classes. This suggests that the values of the V integral calculated by Herrero et al. (1990) are systematically too small (negative) by about 0.5 mag.

As shown in Figure 5, the BCs for the 47 points in our sample are correlated extremely well with $\log T_{\text{eff}}$ and show little dependence on $\log g$. We fitted the BCs as a linear function of both $\log T_{\text{eff}}$ and $\log g$ and derived the relation

$$\text{BC} = 28.46(\pm 0.16) - 7.08(\pm 0.11) \log T_{\text{eff}} + 0.08(\pm 0.02) \log g. \quad (5)$$

The inclusion of a cross term did not yield a statistically better fit. As can be seen from this equation, the dependence on $\log g$ is extremely weak; the simple relation derived by fitting the BC values as a function of $\log T_{\text{eff}}$ alone,

$$\text{BC} = 27.66 - 6.84 \log T_{\text{eff}}, \quad (6)$$

reproduces the BCs determined from equation (5) to within 0.06 mag over the entire range in $\log T_{\text{eff}}$ and $\log g$ of interest here. Equations (5) and (6) are very similar to the relation determined by Chlebowski & Garmany (1991).

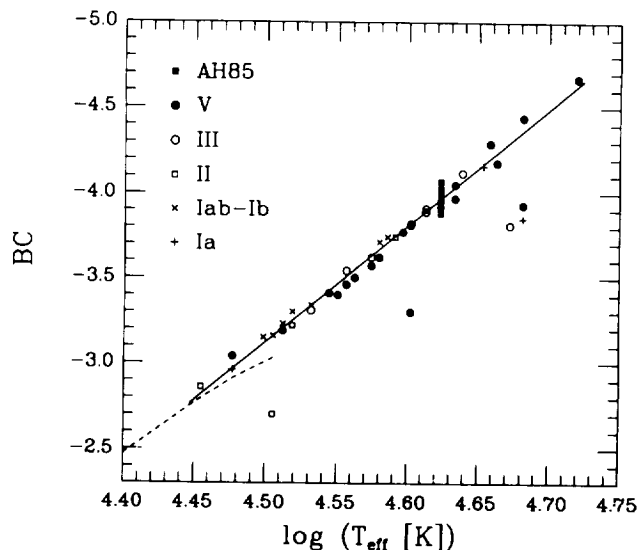


FIG. 5.—The variation of the bolometric correction, BC, with the logarithm of the effective temperature for the stars in the sample. Solid squares denote the results of the models of Abbott & Hummer (1985, marked AH85). The solid line denotes the fit given in eq. (6) to the points. The dashed line represents the relation given by Malagnini et al. (1986).

However, because equation (5) is based on the results from more recent non-LTE models and far more data points and accounts explicitly for variations with $\log g$, we feel it is more reliable than their expression. The BC values calculated from equations (5) and (6) merge smoothly with those determined by Malagnini et al. (1986) at $T_{\text{eff}} \approx 28,000$ K. The BC values determined using equation (5) for specific spectral types and luminosity classes are presented in Tables 5–7.

2.4. M_V Calibration

2.4.1. Previous Calibrations

In order to calibrate absolute visual magnitude as a function of spectral class, both the extinction and the distances to the calibration stars must be known a priori. In the case of O-type stars, distances can be determined only from indirect methods such as main-sequence fitting, which requires a previously established calibration of M_V with intrinsic color $(B-V)_0$ for lower mass ZAMS stars (e.g., Blaauw 1963). Numerous calibrations of M_V with either $(B-V)_0$ or spectral type for OB stars can be found in the literature. However, as far as we are aware none of the recent efforts have begun the calibration process with stars such as the Hyades, whose distances can be directly measured via parallax. We will not attempt to summarize all these M_V calibrations. However, one calibration that differs significantly from others in the literature, as well as from that presented here (see below), deserves some discussion.

The calibration of Schmidt-Kaler (1982) consists of values of M_V as a function of luminosity class and spectral type, from O3 to M5, for normal Population I stars and is based on a review of the published literature. Although the Schmidt-Kaler M_V calibration for OB stars was derived from a number of references, some of these simply provide averages of M_V calibrations presented in other references. The only references that can be considered primary are those by Lesh (1968), Walborn (1973), and Balona & Crampton (1974). The results of Lesh (1968) are based on stars in Gould's Belt, which contains very few O-type stars, and therefore the resulting calibration is valid primarily for

B1–B5 stars. The stellar sample used by Balona & Crampton (1974) contains only 12 O stars, 10 of which are of luminosity class V, and none of which are earlier than O6. Given the overlapping nature of the calibrations in the references listed, the small sample of primary data included, and the unknown nature of the method used to construct the M_V calibration, we conclude that the calibration of Schmidt-Kaler (1982) cannot be considered reliable.

2.4.2. A New M_V Calibration

We used the method of main-sequence fitting of several well-observed Galactic OB associations to determine a new M_V calibration for OB stars. Many of the other recent M_V calibrations for O stars are based upon cluster and association distances that were derived from earlier OB star absolute magnitude calibrations (a circular procedure). While there is no evidence of a systematic problem with this method, we made an effort to confirm, via main-sequence fitting, that there is no discontinuity in the variation of M_V with spectral type for O and B stars. We began with the large body of B-star data presented by de Geus, de Zeeuw, & Lub (1989) for the nearest OB association, Scorpio-Centaurus (Sco OB 2), which contains stars as late as A type. In our analysis we adopted the M_V derived for each star by de Geus et al. (1989). Although these values are themselves based on an earlier calibration of absolute magnitudes with photometric colors derived by Straizys & Kuriliene (1981), this calibration has not been used in any of the other recent studies of O-type stars. In addition, the photometric distance determined for Sco OB 2 by de Geus et al. (1989) is in agreement with that determined astrometrically by Jones (1970) using the convergent point method.

To extend our sample to include O spectral types, we used the recent studies of the following Galactic OB clusters: Cyg OB2 (Massey & Thompson 1991), Tr 14 and Tr 16 (Massey & Johnson 1993), and NGC 6611 (Hillenbrand et al. 1993). In each study, UBV CCD photometry was used to identify intrinsically blue stars, for which optical spectra were then acquired and used to determine accurate MK spectral types. The results include magnitudes, colors, and spectral classifications for a substantial number of O and early B-type stars and thus span a much larger interval on the main sequence in the H-R diagram than earlier work. In addition, these papers contain critical examinations of the slope of the reddening law, the value of which is not always discussed or determined in earlier studies of OB associations even though it can have a significant effect on the derived absolute magnitudes. We did not adopt the absolute magnitudes quoted in these three studies for stars with MK spectral types because they are based on the types of calibrations we are trying to improve: Conti et al. (1983) for the O-type stars and Humphreys & McElroy (1984) for the B stars. Rather, we computed the M_V of each star for a range of distance moduli and then the lower main sequence of these clusters to the upper end of the Sco OB 2 data in the H-R diagram. The distance moduli that gave the best fits turned out to be nearly identical to those derived in Massey & Thompson (1991), Massey & Johnson (1993), and Hillenbrand et al. (1993), a result which confirms that there is no overall systematic difference between the M_V calibration presented here and those of Conti et al. (1983) and Humphreys & McElroy (1984). However, there are differences for individual spectral types.

While a data set based on these Galactic clusters alone is sufficient to calibrate M_V for main-sequence O-type stars, it

contains far too few evolved, luminosity class I, II, and III stars for a calibration of their absolute magnitudes. The only source of O supergiants with MK spectral types and well-determined distances is the Large Magellanic Cloud (LMC), although to include LMC stars in our sample we must assume that the absolute magnitude calibration is the same in the LMC as in our Galaxy. We used the published M_V values for stars with MK spectral types in the associations LH 117 and LH 118 (Massey et al. 1989), LH 9 and LH 10 (Parker et al. 1992) and LH 58 (Garmany, Massey, & Parker 1994). Fortunately, these studies of LMC OB associations were carried out in the same manner as for the Galactic clusters. We then added field LMC O-type stars with reliable photometry and MK spectral types in order to increase the number of evolved stars in the sample. These included the O-type stars discussed by Fitzpatrick & Garmany (1990) and the additional O and B-type stars classified by Massey et al. (1995) and listed in their Table 1. We assumed a distance modulus for the LMC of 18.5 (McCall 1993). There does not appear to be any significant discrepancy in M_V between the ZAMS defined by the LMC O stars and that determined from the Galactic O stars. Our final sample contains 338 stars and is sufficiently large to allow us to construct an M_V calibration for all O and early B spectral types and luminosity classes.

The average M_V values computed for each spectral type and luminosity class are presented in Figure 6. Although the standard deviations are quite large (typically about 0.6 mag), the separations between the average absolute magnitudes for the three luminosity classes are readily apparent, as are the variations of the average M_V values with spectral type. Using the same procedure described above for deriving the calibrations for the effective temperature and gravity, we assumed that M_V is a function of both spectral type and luminosity class and determined the best-fit coefficients for the relation

$$M_V = A + B \times S + C \times L_c + D \times S \times L_c. \quad (7)$$

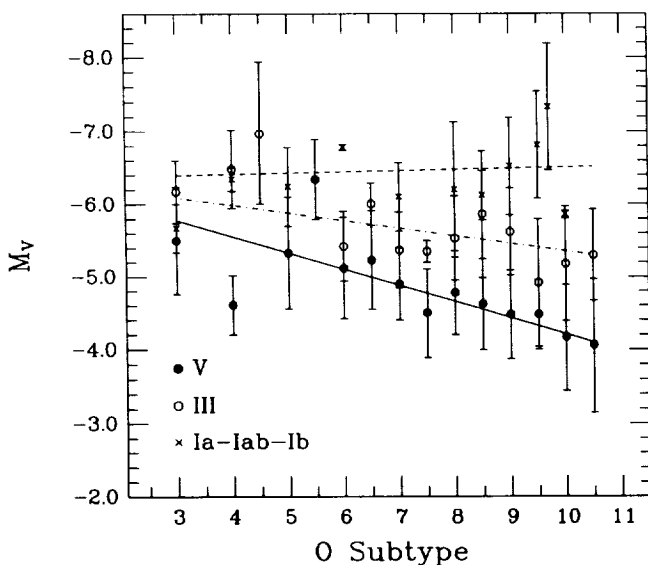


FIG. 6.—Variation of the absolute V magnitude, M_V , with spectral subtype and luminosity class. Points represent the averages determined for each spectral class, and error bars denote the standard deviations. Subtypes 10 and greater refer to B stars. Lines denote the fits determined for three luminosity classes: the solid line is the best fit for luminosity class V stars; the dot-dashed line is for class III stars; the dashed line is for class Ia stars.

Note that we used the individual stellar M_V values to determine the fit coefficients, not the averages shown in Figure 6. In performing the fit, all 338 stars were weighted equally, with $\sigma = 0.5$ mag. The values of the coefficients and their uncertainties are listed in Table 4; the resulting M_V calibrations for three luminosity classes are shown in Figure 6. The rms deviation of the data points from the best fit is about 0.67 mag. The values of M_V calculated for specific spectral types and luminosity classes are presented in Tables 5–7.

3. CALCULATIONS

Unfortunately, we are not able to calibrate the LyC flux from hot stars as a function of spectral type and luminosity class as we did for T_{eff} , $\log g$, and M_V ; the values of q_0 and q_1 , or Q_0 and Q_1 , are rarely reported as results of the non-LTE spectroscopic analyses of individual stars and, in the case of O-type stars, the LyC region of the spectrum has never been observed directly. Furthermore, no extensive and well-sampled grid of q values calculated from the current generation of non-LTE atmosphere models at a large set of $(T_{\text{eff}}, \log g)$ points is presently available. Instead, we must use other model atmospheres to determine q and Q as a function of the stellar parameters. We chose to use the latest models of Kurucz (1992; see also Castelli & Kurucz 1994). Here we describe the method by which we determined the stellar parameters and the ionizing fluxes and luminosities for a given spectral type and luminosity class.

For each spectral class we determined T_{eff} , $\log g$, and M_V from equations (1), (3), and (7), respectively. The bolometric correction was derived from equation (5). The total luminosity L was then computed with the equation

$$\log(L/L_{\odot}) = -0.4(M_V + \text{BC} - M_{\text{bol},\odot}). \quad (8)$$

We adopted $M_{\text{bol},\odot} = 4.75$ mag (Allen 1976) and $\text{BC}_{\odot} = -0.07$ mag (Code et al. 1976); Panagia (1973) used $M_{\text{bol},\odot} = 4.72$ mag, and Schmidt-Kaler (1982) used $M_{\text{bol},\odot} = 4.64$ mag. The values of the luminosity L calculated for specific spectral types and luminosity classes are presented in Tables 5–7. In Figure 7 we plot the temperatures and luminosities derived from our calibrations for O and B stars of luminosity classes V, III, and Ia, on the H-R diagram. The upper mass end of the theoretical ZAMS predicted by the evolutionary calculations of Schaller et al. (1992) is also shown in this figure. The qualitative agreement between the spectroscopic results and the evolutionary calculations is quite good.

The stellar radius R was then determined from the luminosity and the effective temperature with the equation

$$R^2 = \frac{L}{4\pi\sigma T_{\text{eff}}^4}. \quad (9)$$

The stellar mass was determined from the relation

$$M = \frac{gR^2}{G}. \quad (10)$$

This method of determining the mass is made possible by our calibration of $\log g$. Because the value depends only on the parameters determined from atmospheric models applied to spectroscopic data, this mass estimate is referred to as the “spectroscopic mass,” M_{spec} . For the uncertainties in the values of T_{eff} , $\log g$ and M_V listed above, the uncertainty in the stellar radius is about 30%, while the uncer-

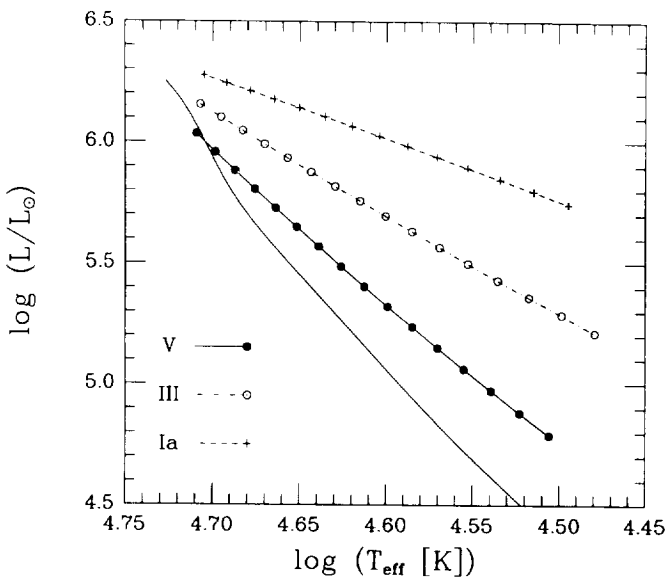


FIG. 7.—The location of O and early B-type stars of three luminosity classes (V, III, and Ia) in the H-R diagram, as derived from our calibrations. The points denote values for the spectral subtypes, at each half-subtype, between O3 and B0.5 (for class V and III stars) and between O3 and O9.5 (for class Ia stars). The solid line denotes the ZAMS in the evolutionary models of Schaller et al. (1992).

tainty in the spectroscopic mass is about 70%. Both values are dominated by the uncertainty in the absolute magnitude.

Alternatively, the stellar mass can be determined from stellar evolution models. For each input temperature and luminosity, we calculated a stellar mass by performing a two-dimensional interpolation on the set of $M(T_{\text{eff}}, L)$ points derived from the evolutionary tracks of Schaller et al. (1992). This estimate of the mass is referred to as the “evolutionary mass,” M_{evol} , which is associated with a value of the stellar gravity, $\log g_{\text{evol}}$. Since the luminosity is a weak function of the gravity (through the bolometric correction), we used the gravity determined from the spectroscopic results ($\log g_{\text{spec}}$) as a first guess for $\log g_{\text{evol}}$, calculated the bolometric correction and luminosity from equations (5) and (8), respectively, and then redetermined M_{evol} and $\log g_{\text{evol}}$. We iterated in this manner until the stellar parameters converged. Throughout our calculations, we assumed the stars were in the first (“redward”) phase of their evolution, moving away from the ZAMS toward lower effective temperatures. In Tables 5–7, we give both the spectroscopic and evolutionary values of the gravity and mass for the various spectral types and luminosity classes. For completeness, we also fitted the values of $\log g_{\text{evol}}$ as a function of spectral type and luminosity class with the expression given in equation (3); the best-fit coefficients A , B , C , and D and their uncertainties are given in Table 4. The evolutionary values of the mass and gravity are found to be systematically larger than the corresponding spectroscopic values. We discuss this “mass discrepancy” at length below (§ 4.3). Fortunately for this study, the values of q_0 and q_1 are only weakly dependent on the value of $\log g$ and therefore are relatively insensitive to variations in the gravity on the order of the difference between $\log g_{\text{spec}}$ and $\log g_{\text{evol}}$, or between $\log g_{\text{eff}}$ and $\log g$.

The theoretical ionizing photon fluxes (photons $\text{cm}^{-2} \text{s}^{-1}$) were computed from the solar metallicity ($Y = 0.1$ by

number) models of Kurucz (1992) with the equation

$$q_i = \int_0^{\lambda_{\text{lim}}^{(i)}} \frac{\pi \lambda F_\lambda}{hc} d\lambda. \quad (11)$$

Here q_0 corresponds to $\lambda_{\text{lim}}^{(0)} = 912 \text{ \AA}$, while q_1 corresponds to $\lambda_{\text{lim}}^{(1)} = 504 \text{ \AA}$.⁷ The quantity F_λ is the flux density at wavelength λ , obtained from the Kurucz (1992) model with a given temperature and gravity. We calculated $\log q$ for each available Kurucz (1992) model and constructed grids of $\log q$ values in the $(T_{\text{eff}}, \log g)$ plane. In order to bracket the range of T_{eff} and $\log g$ values found in massive stars and thereby avoid the difficulties involved with extrapolating from the results derived from the Kurucz models alone, we extended the grids to high temperatures, $T_{\text{eff}} > 50,000 \text{ K}$, at all values of $\log g$, with $\log q$ values derived from blackbody spectral distributions. As shown by Leitherer (1990), the blackbody approximation is reasonable and fairly accurate at these high temperatures. Furthermore, at high temperatures the $\log q$ values derived from the Kurucz models are only weakly dependent on the value of the gravity. We confirmed that the $\log q$ values derived from the Kurucz models for $T_{\text{eff}} \leq 50,000 \text{ K}$ merge smoothly with those determined from the blackbody distributions for $T_{\text{eff}} > 50,000 \text{ K}$. We note that the values of q_2 for the He II continuum [$\lambda_{\text{lim}}^{(2)} = 228 \text{ \AA}$] are often several orders of magnitude smaller than those of q_1 for O-type stars. Therefore, the absence of metal absorption edges in the wavelength range $\lambda < 228 \text{ \AA}$ in the smooth blackbody spectral distributions has little effect on the estimated values of q_0 and q_1 .

To compute ionizing fluxes for any given input set of parameters, we performed a two-dimensional bicubic spline interpolation, as a function of $\log T_{\text{eff}}$ and $\log g$, on the extended grids of $\log q$ values. At each point we required that no interpolated value of $\log q_0$ be larger than the corresponding value derived from a blackbody at the same temperature; no upper limit was placed on the interpolated values of $\log q_1$. This method of extending and performing the interpolations on the $\log q$ grids is similar to that used by Vacca (1994). As a result of the assumptions made in the construction of the grids and in the interpolation procedure, we estimate our interpolated values of q , at any given temperature and gravity, are accurate to about 20%. A comparison with alternative interpolation and extrapolation procedures (e.g., Sutherland & Shull 1995) confirms this estimate. For each spectral type and luminosity class the ionizing luminosities Q_i (photons s^{-1}) were then derived from the ionizing photon fluxes q_i with the equation

$$Q_i = 4\pi R^2 q_i. \quad (12)$$

4. RESULTS

4.1. Lyman Continuum Fluxes

In Tables 5–7, we present the values of q_0 , Q_0 , q_1 , and Q_1 , calculated according to the procedures outlined above, for

⁷ We did not compute the value of the He II ionizing flux, q_2 , which corresponds to $\lambda_{\text{lim}}^{(2)} = 228 \text{ \AA}$. Non-LTE atmospheric models incorporating spherical extension and the effects of winds indicate that non-LTE plane-parallel hydrostatic models substantially underestimate (by a factor of ~ 1000) the fluxes in the He II Lyman continuum, $\lambda < 228 \text{ \AA}$ (e.g., Gabler et al. 1992). The plane-parallel hydrostatic LTE models of Kurucz (1992) cannot be reasonably expected to provide good approximations to the fluxes in this regime. Fortunately, even with the large increases in the values of q_2 predicted by the Unified Atmosphere Models, the fluxes at these wavelengths have a negligible contribution to the values of q_0 and q_1 .

TABLE 5
PARAMETERS FOR OB STARS: LUMINOSITY CLASS V

Spectral Type	T_{eff} (K)	$\log g_{\text{spec}}$ (cgs)	$\log g_{\text{evol}}$ (cgs)	M_V (mag)	BC (mag)	$\log L/L_{\odot}$	M_{spec} (M_{\odot})	M_{evol} (M_{\odot})	R (R_{\odot})	$\log q_0$ ($\text{cm}^{-2} \text{s}^{-1}$)	$\log Q_0$ (s^{-1})	R_s (pc)	$\log q_1$ ($\text{cm}^{-2} \text{s}^{-1}$)	$\log Q_1$ (s^{-1})
O3.....	51230	3.907	4.149	-5.78	-4.56	6.035	51.3	87.6	13.2	24.85	49.87	6.16	24.16	49.18
O4.....	48670	3.905	4.106	-5.55	-4.40	5.882	44.2	68.9	12.3	24.74	49.70	5.41	24.03	48.99
O4.5.....	47400	3.904	4.093	-5.44	-4.32	5.805	41.0	62.3	11.8	24.68	49.61	5.06	23.97	48.90
O5.....	46120	3.903	4.081	-5.33	-4.24	5.727	38.1	56.6	11.4	24.62	49.53	4.72	23.91	48.81
O5.5.....	44840	3.902	4.060	-5.22	-4.15	5.647	35.5	50.4	11.0	24.56	49.43	4.40	23.85	48.72
O6.....	43560	3.901	4.042	-5.11	-4.06	5.567	33.1	45.2	10.7	24.50	49.34	4.09	23.77	48.61
O6.5.....	42280	3.901	4.030	-4.99	-3.97	5.486	30.8	41.0	10.3	24.42	49.23	3.78	23.68	48.49
O7.....	41010	3.900	4.021	-4.88	-3.88	5.404	28.8	37.7	10.0	24.34	49.12	3.47	23.56	48.34
O7.5.....	39730	3.899	4.006	-4.77	-3.78	5.320	26.9	34.1	9.6	24.25	49.00	3.16	23.41	48.16
O8.....	38450	3.898	3.989	-4.66	-3.68	5.235	25.1	30.8	9.3	24.15	48.87	2.86	23.20	47.92
O8.5.....	37170	3.897	3.974	-4.55	-3.58	5.149	23.6	28.0	9.0	24.03	48.72	2.56	22.93	47.63
O9.....	35900	3.896	3.959	-4.43	-3.47	5.061	22.1	25.4	8.8	23.89	48.56	2.26	22.58	47.25
O9.5.....	34620	3.895	3.947	-4.32	-3.36	4.972	20.8	23.3	8.5	23.73	48.38	1.96	22.12	46.77
B0.....	33340	3.894	3.932	-4.21	-3.24	4.881	19.5	21.2	8.3	23.54	48.16	1.65	21.61	46.23
B0.5.....	32060	3.894	3.914	-4.10	-3.12	4.789	18.4	19.3	8.0	23.30	47.90	1.35	21.09	45.69

all O spectral types and the three major luminosity classes. Plots of Q_0 as a function of both spectral type and T_{eff} , for the three luminosity classes, are presented in Figure 8. Similar plots for Q_1 are given in Figure 9. Plots of Q_0 as a function of spectroscopic mass and evolutionary mass are presented in Figure 10. In Figure 11a we compare the values of $\log Q_0$ given by Panagia (1973) with those derived here. As shown in this figure, our values are often a factor of 2 larger; at B0.5 our values are larger than Panagia's (1973)

by nearly a factor of 30. The differences between the two sets of values are primarily due to the differences in the temperature calibrations, as can be seen by comparing the shapes of the curves in Figure 3a and Figure 11a. In Figure 11b we compare the $\log Q_0$ values given by Leitherer (1990) with our values. Here the differences are much smaller, despite the fact that Leitherer (1990) relied on the calibrations of T_{eff} and M_V given by Schmidt-Kaler (1982). Because Leitherer (1990) used the models of Kurucz (1979)

TABLE 6
PARAMETERS FOR OB STARS: LUMINOSITY CLASS III

Spectral Type	T_{eff} (K)	$\log g_{\text{spec}}$ (cgs)	$\log g_{\text{evol}}$ (cgs)	M_V (mag)	BC (mag)	$\log L/L_{\odot}$	M_{spec} (M_{\odot})	M_{evol} (M_{\odot})	R (R_{\odot})	$\log q_0$ ($\text{cm}^{-2} \text{s}^{-1}$)	$\log Q_0$ (s^{-1})	R_s (pc)	$\log q_1$ ($\text{cm}^{-2} \text{s}^{-1}$)	$\log Q_1$ (s^{-1})
O3.....	50960	3.827	4.084	-6.09	-4.55	6.154	57.5	101.4	15.3	24.84	49.99	6.75	24.14	49.30
O4.....	48180	3.774	4.005	-5.98	-4.38	6.046	49.7	82.8	15.1	24.72	49.86	6.12	24.00	49.14
O4.5.....	46800	3.748	3.971	-5.93	-4.30	5.991	46.2	75.8	15.0	24.66	49.80	5.81	23.93	49.07
O5.....	45410	3.722	3.931	-5.88	-4.21	5.934	43.1	68.4	15.0	24.59	49.73	5.51	23.85	48.98
O5.5.....	44020	3.695	3.891	-5.83	-4.11	5.876	40.2	62.0	14.9	24.52	49.65	5.21	23.76	48.89
O6.....	42640	3.669	3.855	-5.78	-4.02	5.817	37.5	56.6	14.8	24.45	49.58	4.92	23.65	48.77
O6.5.....	41250	3.643	3.820	-5.72	-3.92	5.756	35.0	52.0	14.8	24.37	49.50	4.62	23.51	48.63
O7.....	39860	3.617	3.782	-5.67	-3.82	5.695	32.8	47.4	14.7	24.29	49.41	4.32	23.34	48.46
O7.5.....	38480	3.590	3.742	-5.62	-3.71	5.631	30.7	43.0	14.7	24.20	49.32	4.03	23.14	48.26
O8.....	37090	3.564	3.700	-5.57	-3.60	5.566	28.8	39.0	14.7	24.11	49.22	3.75	22.89	48.01
O8.5.....	35700	3.538	3.660	-5.52	-3.48	5.499	27.1	35.6	14.7	24.00	49.12	3.46	22.59	47.71
O9.....	34320	3.511	3.621	-5.46	-3.36	5.431	25.5	32.6	14.7	23.85	48.97	3.08	22.24	47.36
O9.5.....	32930	3.485	3.582	-5.41	-3.24	5.360	24.1	29.9	14.7	23.66	48.78	2.66	21.84	46.96
B0.....	31540	3.459	3.542	-5.36	-3.11	5.287	22.7	27.4	14.7	23.43	48.55	2.23	21.34	46.46
B0.5.....	30160	3.432	3.500	-5.31	-2.97	5.211	21.5	25.1	14.8	23.15	48.27	1.80	20.74	45.86

TABLE 7
PARAMETERS FOR OB STARS: LUMINOSITY CLASS Ia

Spectral Type	T_{eff} (K)	$\log g_{\text{spec}}$ (cgs)	$\log g_{\text{evol}}$ (cgs)	M_V (mag)	BC (mag)	$\log L/L_{\odot}$	M_{spec} (M_{\odot})	M_{evol} (M_{\odot})	R (R_{\odot})	$\log q_0$ ($\text{cm}^{-2} \text{s}^{-1}$)	$\log Q_0$ (s^{-1})	R_s (pc)	$\log q_1$ ($\text{cm}^{-2} \text{s}^{-1}$)	$\log Q_1$ (s^{-1})
O3.....	50680	3.747	4.013	-6.40	-4.54	6.274	64.4	115.9	17.8	24.82	50.11	7.39	24.12	49.41
O4.....	47690	3.644	3.928	-6.41	-4.36	6.210	55.9	104.7	18.6	24.70	50.02	6.92	23.96	49.29
O4.5.....	46200	3.592	3.866	-6.42	-4.27	6.176	52.1	95.7	19.1	24.63	49.98	6.67	23.87	49.22
O5.....	44700	3.540	3.800	-6.43	-4.17	6.141	48.6	86.5	19.6	24.56	49.93	6.42	23.77	49.13
O5.5.....	43210	3.489	3.740	-6.44	-4.07	6.104	45.4	79.5	20.1	24.48	49.87	6.16	23.64	49.03
O6.....	41710	3.437	3.690	-6.44	-3.97	6.066	42.5	74.7	20.6	24.40	49.81	5.90	23.49	48.90
O6.5.....	40210	3.385	3.636	-6.45	-3.86	6.026	39.8	69.6	21.2	24.32	49.75	5.63	23.31	48.75
O7.....	38720	3.333	3.577	-6.46	-3.75	5.984	37.4	64.3	21.8	24.23	49.69	5.35	23.11	48.57
O7.5.....	37220	3.282	3.516	-6.47	-3.63	5.940	35.1	59.2	22.4	24.13	49.62	5.06	22.89	48.38
O8.....	35730	3.230	3.456	-6.48	-3.51	5.895	33.1	54.8	23.1	24.03	49.54	4.77	22.64	48.15
O8.5.....	34230	3.178	3.395	-6.48	-3.38	5.847	31.2	50.6	23.8	23.92	49.45	4.47	22.38	47.92
O9.....	32740	3.126	3.333	-6.49	-3.25	5.796	29.5	46.7	24.6	23.77	49.33	4.08	22.03	47.59
O9.5.....	31240	3.075	3.269	-6.50	-3.11	5.743	27.9	43.1	25.4	23.57	49.17	3.59	21.58	47.17

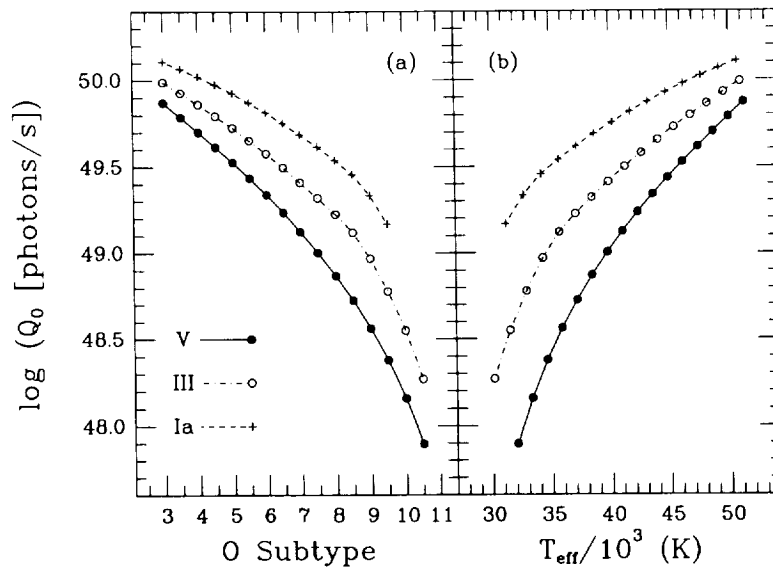


FIG. 8.—The variation of the H ionizing photon luminosity, Q_0 , with (a) spectral subtype and (b) effective temperature for three major luminosity classes. The points denote values for the spectral subtypes, at each half-subtype, between O3 and B0.5 (for class V and III stars) and between O3 and O9.5 (for class Ia stars). Subtypes 10 and greater refer to B stars.

in his calculations, the differences between our values of Q_0 and his are primarily due to the differences between our calibrations for T_{eff} and M_V (§ 2) and those of Schmidt-Kaler (1982).

For the earliest subtypes, the values of Q_0 , Q_1 , and the ratio Q_1/Q_0 derived from our calculations are very close to those determined from blackbody spectral energy distributions. This is due to the fact that we assumed that both q_0 and q_1 approach their respective blackbody values at high T_{eff} . Although this assumption appears to be reasonable for these integrals of the flux (and stabilizes the interpolation procedure on the grids of $\log q$ values), it does *not* imply that the actual stellar flux distributions as a function of wavelength, $F_\lambda(\lambda)$, approach a blackbody shape. To provide further justification for our assumptions and methods, we attempted to confirm that the ionizing fluxes determined from our procedures were similar to and consistent with

those determined from various models constructed specifically for hot stars.

We compared our values of the LyC fluxes (q_0) with those derived from the non-LTE, plane-parallel hot star atmosphere models computed by Husfeld et al. (1984), Abbott & Hummer (1985), Clegg & Middlemass (1987), and Voels et al. (1989). These models include only H and He and therefore do not account for additional opacity in the Lyman continuum due to the presence of metals. Some of the models incorporate mass loss through a stellar wind and the effects of wind blanketing. In general, the agreement between our estimates of q_0 and those computed from these models was found to be better than about 20%.

We also compared our q_0 values with those from the non-LTE atmosphere models of Kudritzki et al. (1991) and Kunze et al. (1992, 1994, private communication). These models are plane-parallel and hydrostatic, and account for

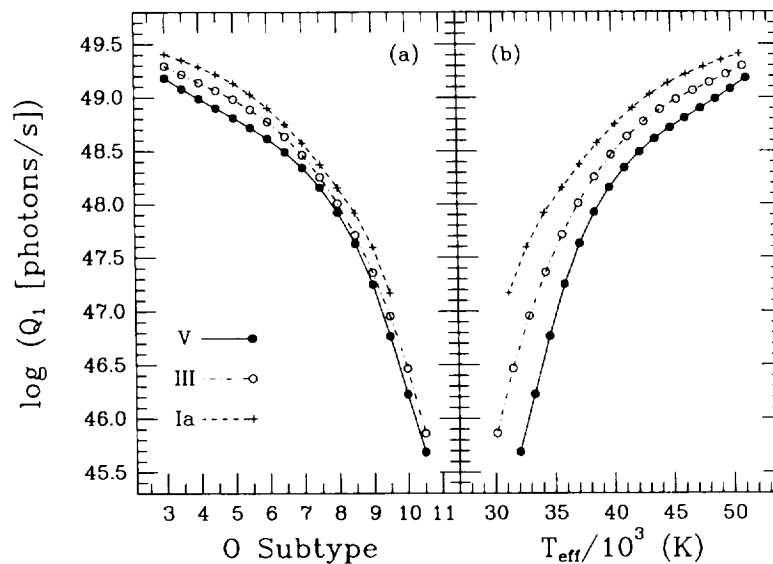


FIG. 9.—The variation of the He ionizing photon luminosity, Q_1 , with (a) spectral subtype and (b) effective temperature for three major luminosity classes. The points denote values for the spectral subtypes, at each half-subtype, between O3 and B0.5 (for class V and III stars) and between O3 and O9.5 (for class Ia stars). Subtypes 10 and greater refer to B stars.

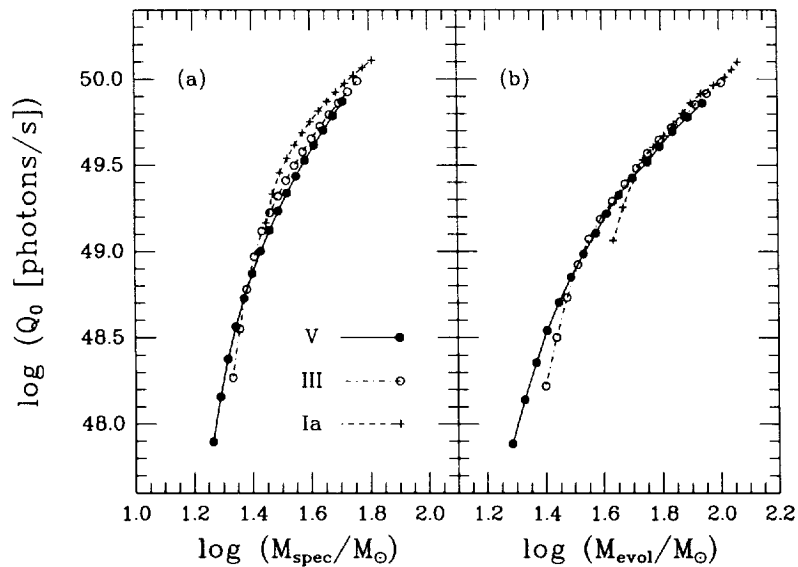


FIG. 10.—The variation of the H ionizing photon luminosity, Q_0 , with (a) spectroscopic mass M_{spec} and (b) evolutionary mass M_{evol} for three major luminosity classes. The points denote values for the spectral subtypes, at each half-subtype, between O3 and B0.5 (for class V and III stars) and between O3 and O9.5 (for class Ia stars).

the effects of wind blanketing and CNO (as well as H and He) opacities on the emergent fluxes. For class V stars with temperatures between 35,000 and 51,000 K and gravities of $\log g = 4.0$, the q_0 values presented by Kudritzki et al. (1991) agree with our values to better than about 20%. Our values were found to be systematically larger, with the largest discrepancy occurring at the *lowest* temperature. For class I stars with the same temperatures, the agreement was within 25%; here our values were systematically smaller, but again the largest discrepancy occurred at the lowest temperature. Similar results and levels of agreement were found upon comparing our values with those determined from the models provided by Kunze et al. (1992) over the ranges in temperature and gravity appropriate to the stars in this study; again, the discrepancy between the two sets of values was largest for the lowest temperatures considered.

A comparison between the values of q_1 derived from the Kudritzki et al. (1991) models and those presented here reveals that our values are systematically smaller by factors between 1.3 and 2.6 for class V stars. For class I stars, our q_1 values derived from the Kurucz models are systematically smaller by factors of 2–6. Similar factors were found when we compared our values of q_1 with those calculated from the Kunze et al. (1992) models, although the discrepancies were no longer systematic. For certain combinations of T_{eff} and $\log g$, the Kurucz models yield substantially *larger* values of q_1 than the Kunze et al. (1992) models.

We also compared our estimates of q for one particular set of stellar parameters with those computed by Schaerer & Schmutz (1994) from a hydrodynamic non-LTE line-blanketed model. The model of Schaerer & Schmutz (1994) was calculated for the stellar parameters derived for ζ Puppis by Bohannon et al. (1990) ($T_{\text{eff}} = 42,000$ K, \log

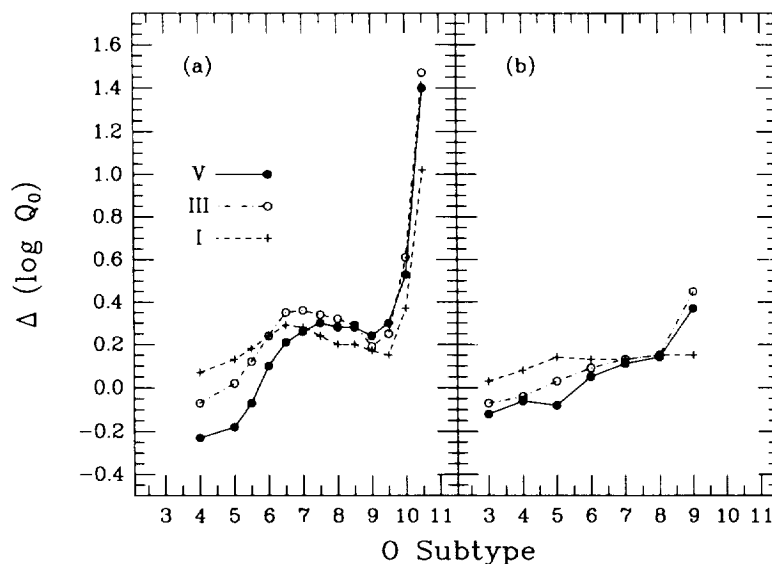


FIG. 11.—Comparison of $\log Q_0$ values derived in this paper with those given by (a) Panagia (1973) and (b) Leitherer (1990) as a function of OB subtype for three luminosity classes. We assumed that the values given in the references for luminosity class I refer to the subclass Ia. Subtypes 10 and greater refer to B stars. Here $\Delta(\log Q_0) = \log Q_0(\text{this paper}) - \log Q_0(\text{reference})$.

$g = 3.5$) and yields $\log q_0 = 24.41$ and $\log q_1 = 23.86$. For the same parameters, we find $\log q_0 = 24.42$ and $\log q_1 = 23.54$. The two values of q_0 agree within 5%; our value of q_1 is about a factor of 2 smaller.

In summary, we believe that our values of q_0 agree within about 25% with those derived from the current generation of non-LTE models used to analyze the spectra of O and early B-type stars. Surprisingly, the agreement is better at higher temperatures. These results appear to justify our use of blackbody energy distributions at high T_{eff} . Our values of q_1 are roughly a factor of 2 smaller than those determined from these non-LTE models. When improved hot star atmosphere models, incorporating the effects of non-LTE, spherical extension, line blanketing, wind emission, and wind blanketing, become widely available and are applied to a large sample of OB stars, the calibrations of T_{eff} and $\log g$ presented here will have to be reevaluated, and the values of q_0 and, in particular, q_1 will have to be recalculated. While the LyC fluxes derived from the Unified Model Atmospheres (e.g., Gabler et al. 1992) or line-blanketed hydrodynamic models (e.g., Schaerer & Schmutz 1994) may not differ substantially from the values presented here for a given T_{eff} and $\log g$, the slightly lower effective temperatures and higher gravities expected from these new models for stars of any given spectral class (see below) imply that the LyC fluxes for each spectral class will decrease slightly. The precise amount by which the q_0 values will change, however, is not yet known. At present, we have to be content with the Kurucz models and be aware of their approximate nature.

Of course, the best means of evaluating the accuracy and reliability of the ionizing fluxes presented here is to compare the values with actual observations of individual stars. Unfortunately, direct observations of the Lyman continuum spectral region are currently available for only two hot stars, β CMa (B1–III) and ϵ CMa (B2 II), both of which have spectral classifications outside the range discussed in this paper. Curiously, the observations yield ambiguous results. Observations of ϵ CMa with the *ROSAT* Wide Field Camera (Hoare, Drew, & Denby 1993) and the *Extreme Ultraviolet Explorer* (*EUVE*) (Cassinelli et al. 1995a) indicate that the LyC flux of this star is a factor of ~ 30 larger than that predicted by both the LTE line-blanketed model atmospheres of Kurucz (1992) and the non-LTE line-blanketed models of Hubeny (1988) and Hubeny & Lanz (1992) for the assumed set of intrinsic stellar parameters ($T_{\text{eff}} = 21,000$ K, $\log g = 3.2$). On the other hand, *ROSAT* observations of β CMa (Hoare et al. 1993) yield count rates which are broadly consistent with the LyC flux predicted by both the Kurucz (1992) models and the non-LTE unblanketed models of Mihalas (1972), even though this star has a higher effective temperature than ϵ CMa.

Cassinelli et al. (1995b) have recently completed an analysis of the spectrum of β CMa obtained with *EUVE* in the wavelength range 500–700 Å. After combining the *EUVE* spectrum with ultraviolet, optical, and infrared observations, these authors find that neither the LTE models of Kurucz (1992) nor the non-LTE models of Hubeny & Lanz (1992) can provide a consistent representation of the observed spectral energy distribution of this star over all wavelength ranges. They derive two sets of stellar parameters ($T_{\text{eff}} = 24,800$ K, $\log g = 3.7$ and $T_{\text{eff}} = 23,250$ K, $\log g = 3.5$), depending on which set of observations they attempt to fit. A Kurucz (1992) model with the larger value

of T_{eff} yields good agreement with the observed LyC and ultraviolet fluxes, while a model with the lower T_{eff} underestimates the observed flux in the Lyman continuum by a factor of ~ 5 . Unfortunately, this ambiguity in the results for β CMa precludes any definitive conclusions regarding the agreement between the models and the observations. Nevertheless, it is clear that in the case of β CMa a huge discrepancy between the observed LyC flux and that predicted by the Kurucz (1992) models, as was found for ϵ CMa, is *not* evident. The fact that the discrepancy between the observations and the Kurucz (1992) models is larger for the later type B star is somewhat surprising. Until further observations of the Lyman continua of hot stars are obtained, no firm conclusions regarding the reliability of the Kurucz (1992) models as applied to O and early B-type stars can be drawn from the results for these two B stars.

4.2. Strömgren Radii

For any star, the radius of the “Strömgren sphere,” denoting the volume of nearly complete ionization of a uniform-density pure H medium surrounding the star, can be easily calculated from

$$R_s = \left(\frac{3Q_0}{4\pi n_H^2 \alpha_B} \right)^{1/3}, \quad (13)$$

where n_H is the H number density per unit volume and α_B is the “case B” rate coefficient for recombination to all levels above the ground level (Osterbrock 1989). In a uniform-density medium, with $n_H = (100 \text{ cm}^{-3})n_{100}$ and an electron temperature of $T = 10^4$ K, values typical of H II regions, we have

$$R_s = 3.16(Q_0/10^{49} \text{ s}^{-1})^{1/3} n_{100}^{-2/3} \text{ pc}, \quad (14)$$

where we have scaled Q_0 by the value appropriate for an O7.5 V star. Strömgren radii are listed for each spectral class in Tables 5–7.

4.3. Masses and the Mass Discrepancy

Both the spectroscopic masses (M_{spec}) and the evolutionary masses (M_{evol}) are listed in Tables 5–7 for stars of specific spectral types and luminosity classes. In Figure 12a we plot the ratio $M_{\text{evol}}/M_{\text{spec}}$ versus O subtype for luminosity classes V, III, and Ia. The difference between the two mass estimates is systematic (the evolutionary masses are systematically larger than the spectroscopic masses) and substantial (approaching factors of 2), particularly for the earliest subtypes. This systematic difference between the values of M_{spec} and M_{evol} is known as the “mass discrepancy.” Herrero et al. (1992) found a similar discrepancy in their analysis of Galactic O-type giant and supergiant stars and gave a detailed discussion of the possible causes. However, contrary to the results of Herrero et al. (1992), but in agreement with those obtained by Groenewegen, Lamers, & Pauldrach (1989), we find that the mass discrepancy occurs in *all* luminosity classes, including luminosity class V. The magnitude of the mass discrepancy found by Groenewegen et al. (1989) is nearly identical to that found here.

The mass discrepancy cannot be attributable solely to a problem in the T_{eff} determinations, as systematic reductions in the effective temperatures on the order of 10,000 K (and substantially more in many cases) would be required to bring the two mass estimates into agreement. Such a large error in the spectroscopic temperature determinations seems unlikely. Furthermore, for any *given* T_{eff} and spectral

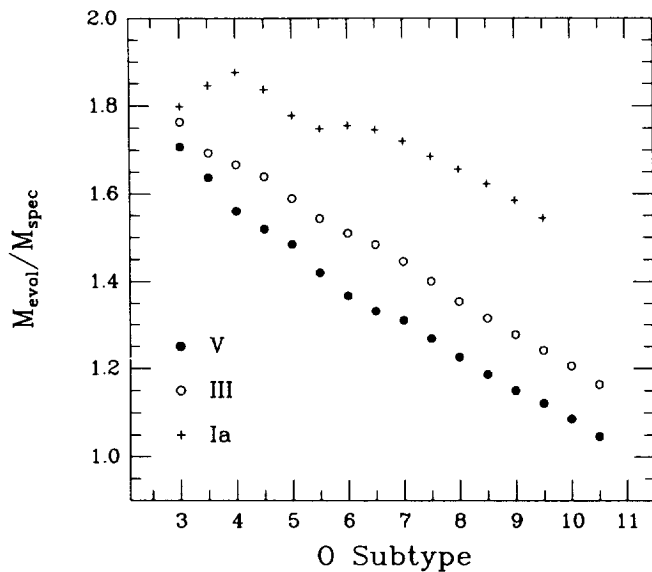


FIG. 12a

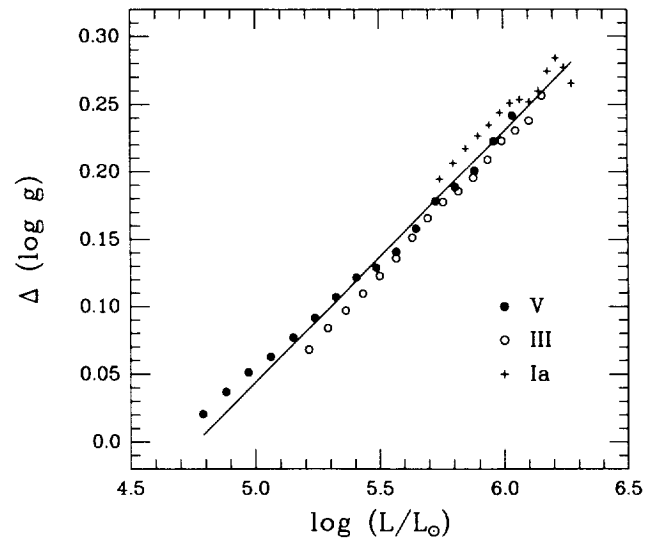


FIG. 12b

FIG. 12.—(a) The “mass discrepancy,” expressed in terms of the ratio of evolutionary and spectroscopic masses, is plotted vs. O subtype. (b) The difference between the values of stellar gravity derived from the evolutionary models ($\log g_{\text{evol}}$) and those derived from the atmosphere models ($\log g_{\text{spec}}$) is plotted vs. the logarithm of the stellar bolometric luminosity for three major luminosity classes; here $\Delta(\log g) = \log g_{\text{evol}} - \log g_{\text{spec}}$. The points denote values for the spectral subtypes, at each half-subtype, between O3 and B0.5 (for class V and III stars) and between O3 and O9.5 (for class Ia stars). The solid line is the best linear fit to all the points and has a slope of 0.19.

classification, the values of BC, L , and R determined from the spectroscopic analysis and the evolutionary models are nearly identical. Thus, the mass discrepancy found at any particular value of T_{eff} must be caused primarily by the different values of the gravity determined from the stellar atmosphere models and from the evolutionary models. Note that the effective gravity determined from model fits to the photospheric lines in the spectra of hot stars is not necessarily equal to the true stellar gravity. Owing to the levitating effects of the wind (and ultimately, the strong radiation pressure which drives the wind), the effective gravity is expected to be reduced with respect to the true gravity for O and early B-type stars.

In Figure 12b we plot the difference between the evolutionary and spectroscopic values of $\log g$ versus the stellar luminosity for spectral types between O3 and B0.5 and luminosity classes V, III, and Ia. The maximum value of the discrepancy in $\log g$ varies with luminosity class but is always less than 0.3. More importantly, the discrepancy is clearly a function of the stellar luminosity, increasing as the stellar luminosity increases, with a functional dependence on luminosity that is approximately the same for all luminosity classes. A linear fit to all the points in Figure 12b yields a slope of 0.19; that is, $\Delta \log g = 0.19 \log(L/L_{\odot}) + \text{Constant}$. Although the luminosity class III points fall systematically below the best fit, and the class Ia points fall systematically above it, all three classes exhibit the same trend and similar slopes. This again suggests that the cause of the discrepancy lies primarily with the atmosphere models, which do not account for physical extension, mass outflow, and velocity fields in stellar winds. As the stellar luminosity increases, the effects of the radiation-driven winds should play a larger role in determining the emergent stellar spectrum.

The results of improved atmosphere models incorporating spherical extension and stellar winds (Gabler et al. 1989; Sellmaier et al. 1993; Schaerer & Schmutz 1994; Herrero et al. 1995) support the suggestion that the current

generation of non-LTE plane-parallel hydrostatic atmosphere models used to perform the spectroscopic analyses of hot stars may be primarily responsible for the mass discrepancy problem. The combination of spherical extension, line blanketing, wind emission, and wind blanketing can have significant effects on the structure of the atmosphere and the predicted emergent spectrum; parameters derived from models that do not incorporate these effects may be substantially in error. Using the Unified Model Atmospheres, which incorporate a radiation driven wind as part of a non-LTE spherical model of hot star atmospheres, Gabler et al. (1989) found that the $\text{H}\gamma$ absorption line profile, normally used to determine $\log g$ for a star, can be affected significantly by wind emission. The wind emission partially fills in the $\text{H}\gamma$ line and causes the emergent line profile to appear narrower and shallower than if the line were purely photospheric in origin (i.e., if a wind were not present). Schaerer & Schmutz (1994) found similar contamination of photospheric lines by wind emission in their spherically extended hydrodynamic line-blanketed models. These results imply that the present generation of plane-parallel hydrostatic models may underestimate the true stellar gravity and mass of the hottest stars with dense winds by about 0.10–0.15 dex. Sellmaier et al. (1993) and Pauldrach et al. (1994) confirm this finding for the O4 I star ζ Puppis; Herrero et al. (1995) find similar results for the O9 Iab star HDE 226868.

It should be noted that Schaerer & Schmutz (1994) found that all photospheric lines are affected somewhat by the presence of a wind. Therefore, fits of plane-parallel models without winds to observed He I and He II line profiles may also yield overestimates of the effective temperatures. Wind blanketing (backscattering of photons into the photosphere by the stellar wind) can also lower the effective temperature estimated for a star, perhaps by several thousand degrees, although the exact amount of the decrease is presently unclear (KH90). If the comparison between the results of Grigsby et al. (1992) and the temperature calibration pre-

TABLE 8
 LYMAN-CONTINUUM LUMINOSITY FROM O STARS IN THE SOLAR NEIGHBORHOOD^a

SPECTRAL TYPE	LUMINOSITY CLASS							
	V-IV		III-II		I		V-I (Total)	
	N	Q_0	N	Q_0	N	Q_0	N	Q_0
O3	1	0.74	0	...	1	1.28	2	2.03
O4	5	2.52	2	1.46	3	3.16	10	7.13
O5	5	1.68	4	2.13	6	5.05	15	8.86
O5.5	5	1.36	2	0.90	0	...	7	2.26
O6	13	2.83	2	0.76	5	3.09	20	6.68
O6.5	16	2.74	8	2.51	3	1.62	27	6.87
O7	27	3.58	11	3.32	7	3.12	45	10.03
O7.5	9	0.91	11	2.29	3	1.14	23	4.34
O8	41	3.04	8	1.57	7	2.25	56	6.87
O8.5	16	0.85	2	0.26	3	0.76	21	1.87
O9	57	2.20	19	1.92	5	0.97	81	5.09
O9.5	56	1.52	30	2.21	21	2.74	107	6.48
O9.7	0	...	1	0.08	14	1.46	15	1.53
Total	251	23.97	100	19.40	78	26.64	429	70.01

^a Total Lyman-continuum photon luminosities Q_0 (in units of 10^{50} s^{-1}) for 429 O-type stars within a distance of 2.5 kpc of the Sun. Also listed are the numbers of stars, N , of luminosity classes V-IV, III-II, and I (Garmany & Vacca 1995).

sented here (§ 2.1.2) is indicative, line blanketing may have the same effect. Indeed, the non-LTE line-blanketed hydrodynamic models of Schaerer & Schmutz (1994) indicate that, for a given mass-loss rate and velocity structure in the wind, the effects of line blanketing on the theoretical H and He absorption line profiles are quantitatively similar to those produced by wind blanketing in the models of Abbott & Hummer (1985) and Bohannan et al. (1986, 1990). However, the results of Schaerer & Schmutz (1994) also indicate that the mass-loss rate and velocity field in the wind can also have significant effects on the profiles of the photospheric H and He lines, and these effects are of the same order as those produced by the line blanketing. Therefore, there is some uncertainty in both the magnitude and the direction of the changes in T_{eff} and $\log g$ (and hence, mass) between the values determined with the current generation of models and those found with models which correctly incorporate the full effects of stellar winds. It may be necessary to redetermine the calibrations of T_{eff} and $\log g$ with spectral class and reexamine the masses and the mass discrepancy problem when newer generations of models, which incorporate the physical effects mentioned above, are applied to a large sample of hot stars.

An alternative explanation for the mass discrepancy is that the mass-loss rates used in the evolutionary models are systematically too small at high luminosities. Increasing the mass-loss rates would result in smaller stellar masses at any given point in the H-R diagram. However, the effects of the increased mass-loss rates on the estimated evolutionary masses of luminosity class V stars would be expected to be extremely small. Nevertheless, we investigated the possibility that the latest evolutionary tracks of Maeder & Meynet (1994) might reduce the mass discrepancy. These new tracks incorporate mass-loss rates in the main-sequence phase which are a factor of 2 larger than those used in the evolution models of Schaller et al. (1992). Although the evolutionary masses of supergiants calculated with the new tracks were indeed found to be systematically smaller than those listed in Table 7 (which were calculated with the tracks from Schaller et al. 1992), the decrease is not nearly enough to resolve the mass discrepancy. Further-

more, the reductions in the masses of luminosity class V and III stars are negligible. Clearly, the mass-loss rates would have to be increased substantially more than a factor of 2 if they are the cause of the mass discrepancy.

However, the combination of the revised mass tracks and the more sophisticated model atmospheres *may* resolve the mass discrepancy. The decreased temperatures, increased gravities, and increased mass-loss rates expected from improved models of hot stars will probably bring the masses derived from the spectroscopic analysis and those derived from the evolutionary tracks into agreement.

4.4. Ionizing Luminosity from Galactic O Stars

As a first application of our results for the LyC luminosities of hot stars, we computed the total ionizing luminosity from a sample of O stars in the solar neighborhood. The total LyC photon luminosity Q_0^{Tot} (s^{-1}) and the LyC areal production rate Ψ_{LyC} ($\text{cm}^{-2} \text{ s}^{-1}$) for the region within 2.5 kpc of the Sun are quantities of interest for models of the ionizing flux in the Galactic disk (Reynolds 1984; Dove & Shull 1994). For example, the diffuse Galactic H α emission observed at high Galactic latitudes requires an ionizing photon flux of $2 \times 10^6 \text{ cm}^{-2} \text{ s}^{-1}$ outward from each side of the Galactic disk into the halo to maintain the emitting gas at an equilibrium ionization state at $T \approx 10^4 \text{ K}$ (Reynolds 1984). Of the many possible sources of ionizing radiation, only O stars appear to produce sufficient LyC flux to account for the observed H α emission. The LyC photon flux from O stars in the Galactic disk that is able to ionize gas at high latitudes is approximately equal to $\Psi_{\text{LyC}} \langle f_{\text{esc}} \rangle / 2$, where $\langle f_{\text{esc}} \rangle$ is the mean fraction of ionizing radiation that escapes from both sides of the Galactic H I layer. Dove & Shull (1994) made detailed calculations of the escape fractions, f_{esc} , through "H II chimneys" above OB associations. Using three-component exponential or Gaussian models of the vertical H I distribution, they found $\langle f_{\text{esc}} \rangle \geq 0.14$. They also estimated the local O-star LyC photon production rate, based on preliminary versions of our LyC results and a catalog of known O-type stars within 2.5 kpc of the Sun. They found $Q_0^{\text{Tot}} = 6.15 \times 10^{51} \text{ s}^{-1}$ and an areal production rate $\Psi_{\text{LyC}} = 3.3 \times 10^7 \text{ cm}^{-2} \text{ s}^{-1}$, considerably higher than

the corresponding values derived from the ionizing fluxes given by Panagia (1973).

In our present calculation, we used a list of O-type stars located within 2.5 kpc of the Sun generated from an extension of the work by Garmany & Stencel (1992) on Galactic OB associations in the northern Milky Way. That study reviewed and assessed the memberships and distances of OB associations between Galactic longitude 55° and 150° . Work currently in progress (Garmany & Vacca 1995) will extend this study to cover the rest of the Galactic plane and will yield a convenient list of association and field O stars. A complete discussion of these stars is beyond the scope of this paper; our purpose here is only to estimate the total LyC photon production rate from a sample of stars and compare the result computed using our values of the stellar ionizing luminosities with that derived from the values given by Panagia (1973).

Known OB associations, whose distances were taken either from Garmany & Stencel (1992) or from Humphreys (1978), were used to construct a sample of O stars that are cluster or association members within 2.5 kpc of the Sun. The distances of field stars were derived from spectroscopic parallax, using the absolute magnitude calibration presented in § 2.4 and the assumptions that the intrinsic $B-V$ color of O stars is -0.31 and that the ratio of total to selective extinction is 3.1. Field stars located within 2.5 kpc of the Sun were then added to the sample. The resulting sample of 429 O-type stars was used to compute the total LyC production rate. Table 8 lists the number of O stars of each spectral type and luminosity class and the LyC luminosities (Q_0) produced by each group. In compiling this table, we combined all luminosity class I stars into one group. The same has been done for stars in luminosity classes II and III and for stars in luminosity classes IV and V. Stars without luminosity classifications were assigned to luminosity class V. These 429 stars provide $Q_0^{\text{Tot}} = 7.00 \times 10^{51} \text{ s}^{-1}$ and $\Psi_{\text{LyC}} = 3.74 \times 10^7 \text{ cm}^{-2}$, values which are 47% higher than those computed using the ionizing luminosities given by Panagia (1973) ($Q_0^{\text{Tot}} = 4.77 \times 10^{51} \text{ s}^{-1}$). With our latest calibrations and stellar catalog, the LyC production rates are even higher than those estimated by Dove & Shull (1994).

Since Q_0^{Tot} was estimated from a sample of stars within a distance of 2.5 kpc of the Sun, a corresponding value for the entire Milky Way disk of radius 12 kpc, Q_0^{Gal} , can be obtained by multiplying Q_0^{Tot} by 23; we find $Q_0^{\text{Gal}} = 1.6 \times 10^{53} \text{ s}^{-1}$. The LyC photon luminosity from the entire Galaxy has been estimated to be $Q_0^{\text{Gal}} = (3 \pm 1) \times 10^{53} \text{ s}^{-1}$ (Mezger 1978); recent *COBE* observations of Galactic [N II] 205 μm emission yield a value of $Q_0^{\text{Gal}} = 3.5 \times 10^{53} \text{ s}^{-1}$ (Bennett et al. 1994). Thus, a simple scaling from the local solar vicinity provides a surprisingly good estimate of the Galactic production rate of ionizing photons.

5. CONCLUSIONS

We have presented new calibrations of the effective temperature, gravity, and absolute visual magnitude as a function of spectral type and luminosity class for O and early B-type stars. The calibrations were derived from the recent results of spectroscopic analyses of hot star absorption line spectra with non-LTE models. The results of these models also enable us to determine the dependence of the bolometric correction on effective temperature and gravity. All these calibrations are presented as convenient mathematical formulae. The formulae also allow direct transformations

from T_{eff} and L back to spectral types and luminosity classes, an inversion that should be particularly useful in spectral synthesis codes which combine evolutionary tracks in the H-R diagram with libraries of actual stellar spectra (e.g., Leitherer, Robert, & Drissen 1992; Robert, Leitherer, & Heckman 1993).

The effective temperature correlates well with spectral type; there is little difference in T_{eff} between the various luminosity classes over the subtype range investigated here (Fig. 2). The gravity, on the other hand, provides the distinction between luminosity classes, with the variation in $\log g$ with subtype different for class V stars than for class I stars (Fig. 4). Figures 2 and 4 also reflect the observational fact that it is nearly impossible to differentiate between the various luminosity I subclasses for stars with spectral types earlier than about O6.5; for these spectral types, there is little difference in the effective temperatures or gravities among the luminosity I subclasses. As might be expected, the bolometric correction depends primarily on the effective temperature, although there is a weak dependence on the gravity (Fig. 5).

Using the recent models of stellar evolution calculated by Schaller et al. (1992), the model atmospheres constructed by Kurucz (1992), and our calibrations of T_{eff} , $\log g$, and M_V , we have determined the intrinsic parameters and the H^0 (Lyman continuum) and He^0 ionizing luminosities for O and early B stars. We find LyC luminosities significantly larger than those given by Panagia (1973), particularly for early B-type stars (Fig. 11). This increase in the ionizing luminosities of individual stars results in a 47% increase in the estimated total LyC luminosity from the O star population within 2.5 kpc of the Sun. Hot stars are the sources of the photoionizing radiation responsible for the strong Balmer emission lines seen in the optical spectra of H II regions, H II galaxies, and starburst galaxies. With the ionizing luminosities provided in Tables 5–7 and Figures 8 and 10, more accurate estimates of the number of O and B-type stars in these objects can be determined.

Despite the qualitative agreement regarding the general locations of O and early B-type stars of various classifications in the H-R diagram (Fig. 7) with the evolutionary models of Schaller et al. (1992), we find that the masses determined from the spectroscopic analysis are systematically smaller than those derived from the evolutionary tracks for the hottest stars (Fig. 2a). This “mass discrepancy” applies to all luminosity classes and is a function of the stellar luminosity (Fig. 2b). Although the large discrepancy between evolutionary and spectroscopic masses has been recognized for some time among those who study hot stars (e.g., Groenewegen et al. 1989), it does not appear to be common knowledge among the general astronomical community. In accord with the findings of other studies, we suggest that the current generation of plane-parallel atmosphere models for hot stars is primarily responsible for the discrepancy, and that the recent improvements in these models (e.g., inclusion of spherical extension, metals, line blanketing, and wind effects) will result in substantial progress in eliminating the discrepancy.

The authors would like to thank Phil Massey, Daniel Schaerer, and Ralph Sutherland for numerous discussions, comments, and suggestions and Peter Conti for his comments and encouragement. We are grateful to R. Kudritzki and D. Kunze for providing their recent model atmosphere results. W. D. V. was supported in part by a Hubble Fellow-

ship through grant HF-1026.01-91A, awarded by the Space Telescope Science Institute, which is operated by the Association of Universities for Research in Astronomy for NASA under contract NAS5-26555. W. D. V. also acknowledges partial support from a Beatrice Watson Parrent Fellowship at the Institute for Astronomy, University of Hawaii, C. D. G. acknowledges support from NSF grant

AST 90-15420 to the University of Colorado. J. M. S. was supported by the NASA Astrophysical Theory Program (grant NAGW-766) at the University of Colorado and by the Visitors Program at the Space Telescope Science Institute during the completion of this work. This research has made use of the SIMBAD database, operated at CDS, Strasbourg, France.

REFERENCES

- Abbott, D. C., & Hummer, D. G. 1985, *ApJ*, 294, 286
 Allen, C. W. 1976, *Astrophysical Quantities*, (London: Athlone)
 Auer, L. H., & Mihalas, D. 1972, *ApJS*, 24, 193
 Balona, L., & Crampton, D. 1974, *MNRAS*, 166, 203
 Bennett, C. L., et al. 1994, *ApJ*, 434, 587
 Blaauw, A. 1963, in *Stars and Stellar Systems*, Vol. 3, ed. K. A. Strand (Chicago: Univ. Chicago Press), 383
 Bohannan, B., Abbott, D. C., Voels, S. A., & Hummer, D. G. 1986, *ApJ*, 308, 728
 Bohannan, B., Voels, S. A., Hummer, D. G., & Abbott, D. C. 1990, *ApJ*, 365, 729
 Bradley, P. T., & Morton, D. C. 1969, *ApJ*, 156, 687
 Cassinelli, J. P., et al. 1995a, *ApJ*, 438, 932
 ———. 1995b, *ApJ*, submitted
 Castelli, F., & Kurucz, R. L. 1994, *A&A*, 281, 817
 Chlebowski, T., & Garmany, C. D. 1991, *ApJ*, 368, 241
 Clegg, R. E. S., & Middlemass, D. 1987, *MNRAS*, 228, 759
 Code, A. D., Davis, J., Bless, R. C., & Hanbury Brown, R. 1976, *ApJ*, 203, 417
 Conti, P. S. 1973, *ApJ*, 179, 181
 ———. 1975, in *H II Regions and Related Objects*, ed. T. Wilson & D. Downes (Heidelberg: Springer), 207
 ———. 1988, in *O Stars and Wolf-Rayet Stars*, ed. P. S. Conti & A. H. Underhill (Washington, DC: NASA SP-497), 81
 Conti, P. S., & Alschuler, W. R. 1971, *ApJ*, 170, 325
 Conti, P. S., & Frost, S. A. 1977, *ApJ*, 212, 728
 Conti, P. S., Garmany, C. D., de Loore, C., & Vanbeveren, D. 1983, *ApJ*, 274, 302
 Conti, P. S., & Leep, E. M. 1974, *ApJ*, 193, 113
 de Geus, E. J., de Zeeuw, P. T., & Lub, J. 1989, *A&A*, 216, 44
 Divan, L., & Burnichon-Prévot, M.-L. 1988, in *O Stars and Wolf-Rayet Stars*, ed. P. S. Conti & A. H. Underhill (Washington, DC: NASA SP-497), 1
 Dove, J. B., & Shull, J. M. 1994, *ApJ*, 430, 222
 Fitzpatrick, E. F., & Garmany, C. D. 1990, *ApJ*, 363, 119
 Gabler, R., Gabler, A., Kudritzki, R. P., & Mendez, R. H. 1992, *A&A*, 265, 656
 Gabler, R., Gabler, A., Kudritzki, R. P., Puls, J., & Pauldrach, A. 1989, *A&A*, 226, 162
 Garmany, C. D., Massey, P., & Parker, J. Wm. 1994, *AJ*, 108, 1256
 Garmany, C. D., & Stencel, R. E. 1992, *A&AS*, 94, 211
 Garmany, C. D., & Vacca, W. D. 1995, in preparation
 Grigsby, J. A., Morrison, N. D., & Anderson, L. S. 1992, *ApJS*, 78, 205
 Groenewegen, M. A. T., Lamers, H. J. G. L. M., & Pauldrach, A. W. A. 1989, *A&A*, 221, 78
 Herrero, A. 1994, *Space Sci. Rev.*, 66, 137
 Herrero, A., Kudritzki, R. P., Gabler, R., Vilchez, J. M., & Gabler, A. 1995, *A&A*, 297, 556
 Herrero, A., Kudritzki, R. P., Vilchez, J. M., Kunze, D., Butler, K., & Haser, S. 1992, *A&A*, 261, 209
 Herrero, A., Vilchez, J. M., & Kudritzki, R. P. 1990, in *Properties of Hot Luminous Stars*, ed. C. D. Garmany (San Francisco: ASP), 50
 Hickock, F. R., & Morton, D. C. 1968, *ApJ*, 152, 203
 Hillenbrand, L. A., Massey, P., Strom, S. E., & Merrill, K. M. 1993, *AJ*, 106, 1906
 Hiltner, W. A. 1956, *ApJS*, 2, 389
 Hiltner, W. A., & Morgan, W. W. 1969, *AJ*, 74, 1152
 Hoare, M. G., Drew, J. E., & Denby, M. 1993, *MNRAS*, 262, L19
 Hobbs, L. M., Morgan, W. W., Albert, C. E., & Lockman, F. J. 1982, *ApJ*, 263, 690
 Howarth, I. D., & Prinja, R. K. 1989, *ApJS*, 69, 527
 Hubeny, I. 1988, *Comput. Phys. Commun.*, 52, 103
 Hubeny, I., & Lanz, T. 1992, *A&A*, 262, 501
 Humphreys, R. M. 1978, *ApJS*, 38, 309
 Humphreys, R. M., & McElroy, D. B. 1984, *ApJ*, 284, 565
 Husfield, D., Kudritzki, R. P., Simon, K. P., & Clegg, R. E. S. 1984, *A&A*, 134, 139
 Imhoff, J. 1990, *Diplomarbeit*, Univ. Munich, Germany
 Jones, D. H. P. 1970, *MNRAS*, 152, 231
 Kilian, J., Becker, S. R., Gehren, T., & Nissen, P. E. 1991, *A&A*, 244, 419
 Kolb, M. 1991, *Diplomarbeit*, Univ. Munich, Germany
 Kudritzki, R. P. 1976, *A&A*, 52, 11
 ———. 1980, *A&A*, 85, 174
 Kudritzki, R. P., Gabler, A., Gabler, R., Groth, H. G., Pauldrach, A., & Puls, J. 1989, in *IAU Colloq. 113, Physics of Luminous Blue Variables*, ed. K. Davidson, A. F. J. Moffat, & H. J. G. L. M. Lamers (Dordrecht: Reidel), 328
 Kudritzki, R. P., Gabler, R., Kunze, D., Pauldrach, A. W. A., & Puls, J. 1991, in *Massive Stars in Starbursts*, ed. C. Leitherer, N. R. Walborn, T. M. Heckman, & C. A. Norman (Cambridge: Cambridge Univ. Press), 59
 Kudritzki, R. P., & Hummer, D. G. 1990, *ARA&A*, 28, 303 (KH90)
 Kunze, D., Kudritzki, R.-P., & Puls, J. 1992, in *The Atmospheres of Early-Type Stars*, ed. U. Heber & C. S. Jeffery (Berlin: Springer), 45
 Kurucz, R. L. 1979, *ApJS*, 40, 1
 ———. 1992, in *IAU Symp. 149, The Stellar Populations of Galaxies*, ed. B. Barbuy & A. Renzini (Dordrecht: Kluwer), 225
 Lamers, H. J. G. L. M. 1981, *ApJ*, 245, 593
 Leitherer, C. 1990, *ApJS*, 73, 1
 Leitherer, C., Robert, C., & Drissen, L. 1992, *ApJ*, 401, 596
 Lennon, D. J., Dufton, P. L., Keenan, F. P., & Holmgren, D. E. 1991a, *A&A*, 246, 175
 Lennon, D. J., Kudritzki, R.-P., Becker, S. T., Butler, K., Eber, F., Groth, H. G., & Kunze, D. 1991b, *A&A*, 252, 498
 Lesh, J. R. 1968, *ApJS*, 17, 371
 Maeder, A., & Meynet, G. 1994, *A&A*, 287, 803
 Malagnini, M. L., Morossi, C., Rossi, L., & Kurucz, R. L. 1986, *A&A*, 162, 140
 Massey, P., Garmany, C. D., Silkey, M., & DeGioia-Eastwood, K. 1989, *AJ*, 97, 107
 Massey, P., & Johnson, J. 1993, *AJ*, 105, 980
 Massey, P., Lang, C., DeGioia-Eastwood, K., & Garmany, C. D. 1995, *ApJ*, 438, 188
 Massey, P., & Thompson, A. B. 1991, *AJ*, 101, 1408
 Mathys, G. 1988, *A&AS*, 76, 427
 ———. 1989, *A&AS*, 81, 237
 Matthews, T. A., & Sandage, A. R. 1963, *ApJ*, 138, 30
 McCall, M. L. 1993, *ApJ*, 417, L75
 Mezger, P. G. 1978, *A&A*, 70, 565
 Mihalas, D. 1972, *NCAR Technical Note STR-76* (Boulder: NCAR)
 Morton, D. C. 1969, *ApJ*, 158, 629
 Osterbrock, D. E. 1989, *Astrophysics of Gaseous Nebulae and Active Galactic Nuclei* (Mill Valley: University Science Books)
 Panagia, N. 1973, *AJ*, 78, 929
 Parker, J. Wm., Garmany, C. D., Massey, P., & Walborn, N. R. 1992, *AJ*, 103, 1205
 Pauldrach, A. W. A., Kudritzki, R. P., Puls, J., Butler, K., & Hunsinger, J. 1994, *A&A*, 283, 525
 Remie, H., & Lamers, H. J. G. L. M. 1982, *A&A*, 105, 85
 Reynolds, R. J. 1984, *ApJ*, 282, 191
 Robert, C., Leitherer, C., & Heckman, T. M. 1993, *ApJ*, 418, 749
 Schaerer, D., & Schmutz, W. 1994, *A&A*, 288, 231
 Schaller, G., Schaerer, D., Meynet, G., & Maeder, A. 1992, *A&AS*, 96, 269
 Schmidt-Kaler, T. 1982, in *Landolt-Börnstein, New Series, Group, VI, Vol. 2*, ed. K. Schaifers & H. H. Voigt (Berlin: Springer-Verlag), 1
 Schönberner, D., Herrero, A., Becker, S., Eber, F., Butler, K., Kudritzki, R. P., & Simon, K. P. 1988, *A&A*, 197, 209
 Sellmaier, F., Puls, J., Kudritzki, R. P., Gabler, A., Gabler, R., & Voels, S. A. 1993, *A&A*, 273, 533
 Simon, K. P., Jonas, G., Kudritzki, R. P., & Rahe, J. 1983, *A&A*, 125, 34
 Straizys, V., & Kuriliene, G. 1981, *Ap. Space Science*, 80, 353
 Sutherland, R. S., & Shull, J. M. 1995, *ApJ*, submitted
 Vacca, W. D. 1994, *ApJ*, 421, 140
 Van Citters, G. W., & Morton, D. C. 1970, *ApJ*, 161, 695
 Voels, S. A. 1989, *Ph.D. thesis*, Univ. Colorado
 Voels, S. A., Bohannan, B., Abbott, D. C., & Hummer, D. G. 1989, *ApJ*, 340, 1073
 Walborn, N. R. 1971, *ApJS*, 23, 257
 ———. 1972, *AJ*, 77, 312
 ———. 1973, *AJ*, 78, 1067
 ———. 1976, *ApJ*, 205, 419
 ———. 1982, *AJ*, 87, 1300
 Werner, K. 1988, *A&A*, 204, 159

